We thank the editor and two anonymous referees for the comments and for giving us the opportunity to improve our manuscript. Below are our point-by-point responses to the referees' comments, followed by a revised manuscript showing all track changes made through the major revision. Note: all line numbers are based upon the revised manuscript.

Response to anonymous referees #1.

1. **Restructuring the paper**. In the revised manuscript, we have improved the readability by streamlining the introduction and the objectives of the work, followed by a much clearer separation between the presentation of the framework, the illustrative examples and the discussion, as requested by the reviewer. Any duplication have been carefully handled in the revised manuscript. Specifically, in the introduction, we separated previous HSHM studies, summarized limitations and remaining challenges; proposed the benefits of stochastic approaches and indicator formulation and introduced our proposed statistical framework. We also specified the main objectives of each section (L89-L94; L96-L101; L246-L251; L346-L353). Section 2.5 was added to the manuscript to better demonstrate the advantages and linkages between our statistical framework and Bayesian statistics (L226-L244). We moved the mathematical heavy previous section 4.2 into the Appendix to increase the continuity of section 4. In Figure 4 and 5 and following discussions, we changed the y-axis label from previous $< I_{HSHM}(\boldsymbol{\Omega}^*, \tau) >$ to $P(I_{HSHM}(\boldsymbol{\Omega}^*, \tau) = 1)$ to highlight the probability perspective.

2. **Definition of 'disproportionate'**. Based on the complex nature of HSHMs, it is not practical and beneficial to look for a universal mathematical definition using percentage or proportion. For example, a 60^{th} percentile denitrification rate may trigger HSHM at a riparian site, but may fail to indicate HSHM condition at other sites as other static and/or dynamic factors can also control HSHM occurrences significantly. However, our proposed statistical framework provides a very flexible approach that can incorporate different types of HSHMs through static and dynamic contributors, modeled with indicator random variables and stochastic processes. For example, the permanent control points (as defined by Bernhardt et al., 2017) can be modeled with static-only indicators whereas activated control points will require both static and dynamics indicators. The cutoff values, percentage or proportion are defined by users and can be modified at will, as in equation (1). One can change these quantities based on prior information, risk tolerance or through statistical quantities. For certain HSHMs that have negative influences on ecosystems, thresholds are often introduced in environmental regulations in order to identify levels of contamination above which to consider a site as contaminated. In addition, activation thresholds may be used for chemical reactions that are necessary for biogeochemically driven HSHMs. These changes can be found at L48-L52, L55-L61, L62-L67, L118-L131, L226-L244.

3. **Novelty**. We appreciate the reviewer's recommendations of relevant references and studies. We agree with the reviewer that there are many theoretical, empirical models and experimental approaches dealing with the HSHM dynamics. There are also various approaches to define 'hotness' as summarized in Bernhardt et al. (2017), such as simple comparison to average or matrix; substantial percentage of total flux; outlier in distribution of data; statistically significant difference between or among landscape elements or time periods categorized a priori; and contribution to flux/total area or time (L48-L52). However, most of these quantitative methods are derived based on site-specific data or simulation results, which limits the transferability from one site to other sites; and from one type of HSHM to other types of HSHMs (L54-L55). Thus the challenge is not how we define a single cutoff value for a specific HSHM at a specific site, but rather to develop a statistical framework, capable of handling a generality of cases, and therefore progressing beyond local conditions. From this perspective, our proposed framework is novel and beneficial for future HSHM studies, summarized as follows: (a) With the indicator formulation, the framework is flexible enough to handle different scenarios of cutoff values (see point #2); (b) Our proposed framework is unified and allows us to investigate HSHMs under conditions of uncertainty; (c) Our framework can integrate results from HSHM studies using different approaches, whether results from Monte-Carlo simulations or direct data based quantifications; (d) Probabilities are assigned to the entire domain and time of HSHM concerns and modeled with corresponding stochastic processes; (e) Our framework can be easily integrated with Bayesian concepts such as conditioning as well as utilization of prior information from other sites (L54-L66, L226-L244, L506-L521). Based on the above points, we believe the statistical framework can make contributions to the HSHM community.

Response to anonymous referee #2.

Summary notes:
1. **Why stochastic?** The processes governing the HSHMs are very likely subject to some uncertainty. There may be uncertainty in the parameters and also in the governing equations. This is the reason to adopt a stochastic formulation. In this way, the uncertainty can be modeled and even reduced by taking advantage of the information provided by the data. The mechanism for modeling and reducing uncertainty are built into our approach. For example, we can use prior information from similar sites, and we can use local measurements for conditioning. We have better demonstrated this point in L74-L77.

2. **Defining places in space and time as either being or not being HSHMs**. Our characterization of HSHMs is not binary, because we use probabilities. In our approach, all space and time intervals in the investigated domain are associated with probabilities to be or not to be a HSHM. Notice that the location of the HSs is uncertain due to the combined effect of physical system heterogeneity and limitations in its characterization. In addition, even if the positions of the HSs are known without uncertainty, hot moments may depend on other factors (e.g., solute pathway, retention time), which can also be uncertain.

3. **Arbitrary cutoffs**. In our approach, the cutoffs are defined by the user and can be modified at will. One can change the cutoff values based on prior information and based on risk tolerance. For HSHMs that have negative influences, thresholds are often introduced in environmental regulations in order to identify levels of contamination above which to consider a site as contaminated. In addition, activation thresholds may be used to identify the thresholds for reactions that are necessary for biogeochemical driven HSHMs (see also point 5 below).

4. **Binary view of HSHMs.** As stated in point 2, we model the HSHMs stochastically. For example, we can have a zone with high probability next to other zones with lower probabilities in terms of HSHMs occurrence. Thus, we do adopt a continuum approach by creating HSHM probability maps. In another note, we suggest that there might be situations that require focusing on a particular area because of a need to focus on the site investigation efforts. Thus, in our approach, we can identify areas that are more critical/sensitive compared to others, and this could assist the project managers in defining priorities. For example, at the Rifle site (Wainwright et al. 2010), geophysical datasets indicated the presence of naturally reducing zones (NRZs), which may have higher level of uranium and nitrate. Based on this information, site investigation and parameter estimation were both goal oriented, which reduces efforts and uncertainties in quantifying the corresponding HSHMs.

5. **Improving understanding**. We expanded our discussion in order to improve understanding. In particular, we make the following points: (a) Our framework can be used to investigate HSHM sites and identify the process and parameters controlling the HSHMs. (b) As the reviewer noted, there's uncertainty associated with the HSHMs. Using our approach, we can identify which models and parameters work, using for example Bayesian model comparison and identifying the best performing models or whether the current understanding of a certain HSHM is lacking. (c) The probabilistic approach offers great advantages of addressing the uncertainty on HSHMs and reducing it. (d) We will also add information on where to get the threshold parameters.

6. **Why a statistical framework**? Based on the experiences in the hydrology community, the coupling of probabilistic concepts with the physics led to a tremendous progress in our ability to model the complex phenomena taking place in the subsurface. Similar observations have been made on multiple disciplines within earth sciences. There is a vast body of knowledge accumulated in hydrology and what we want to show in this paper is that this knowledge could also bring enormous potential to HSHMs investigations.

7. **Simple language**. We added plain language discussion in the revised manuscript.

Detailed responses:
L40: I am having a hard time with the definition used for HSHM as it depends on the event having a negative effect on something (health or environment). But what if a HSHM does something beneficial like remove a pollutant. Is that not considered here? Maybe a slight modification of the definition is all that's needed.

Response: We modified the definition to include the beneficial perspectives (L35-L39). Table 1 in the revised paper exhibit a column (Impact) indicating whether a specific HSHM has a positive, neutral or negative impact on the ecosystem.

L90: Here again the focus is on the negative side of HSHMs, I suggest taking a more balanced view that includes their benefits as well.

Response: We expanded the HSHM definition to cover both positive and negative perspectives of HSHMs. Please also see our response to L40 comment.

L100: I would suggest adding 1 sentence providing a non-jargon definition of indicator statistics. It will make the work more accessible.
Response: We have made necessary modifications to make the reading more accessible. Technical discussions about indicator statistics are currently presented in Section 2 rather than the introduction. We have also better defined $\boldsymbol{\Omega}^*$, t^* and the indicator random variable in L105-L108.

L135: While I appreciate the development of a rigorous statistical framework, I question the utility of the binary definition of whether a place/time is or is not a HSHM. Do we care more about the definition or its influence? The influence is some continuous function of the magnitude to which it deviates from background conditions. It would be more powerful to define a statistical framework that captured this more continuous perspective. At a minimum, I think the authors should discuss the limitation of their framework and provide ideas for developing a more continuous approach. For example, maybe one could continuously vary the Cth and Rth from equation 1 to examine outcomes across a continuum of thresholds?

Response: As discussed in items 2, 3 and 4 above, our framework is flexible as it can incorporate different conditions that trigger HSHMs. The cutoff values are chosen by users and can be modified at will. With this flexibility, one could definitely vary C_{th} and R_{th} values, and examine how the probability of HSHM occurrences changes correspondingly, as suggested by the Reviewer (L118-L131). Thus our approach indeed captures the continuous perspectives as specified in the previous answers.

L145-L150: All examples are for concentrations (Cth). It would be good to provide some examples for rates (Rth).

Response: In the revised manuscript, we included multiple examples for rates. For example, $R_{th} = 0$ can be used for chemical reactions that have significant negative impact on ecosystem (e.g., nuclear reactions). R_{th} values can also be obtained based on similar studies, such as denitrification and carbon cycling rates summarized in Harms and Grimm (2008). These changes are reflected in L118-L131.

L160: Please briefly explain why type B includes the spatial component instead of only including the temporal.

Response: The idea here is to identify where the dynamic conditions exist in conjunction with spatial zones to trigger a hot spot. For example, following the reviewer's comments, a zone of high concentration may be a location for HSHMs, only that we do not know where it gets triggered. An example here could be nuclear waste remediation sites where natural attenuation strategies are in place. While contaminants can be held in place; within the zones where contamination occurred, yet some temporal conditions may trigger the formation of these HSHMs. Here it is worthwhile to note both the temporal conditions, but also the spatial domain of HS. Furthermore, the hot spot may also depend on variables different from the concentration of the species of original interest. For example, a nuclear contamination site that has historically looked at uranium can now be potential hot spots for strontium.

Equation 3: This seems a bit circular to me. It seems like this says that a location is a hot spot because it has the conditions (e.g., concentration) needed to be a hot spot given our defined threshold of what counts as a hot spot. So it's a hot spot because it's a hot spot. Maybe this can be clarified in terms of how this isn't circular? In other words, explain further why it is useful to call some place a hot spot based on defined criteria. Why don't we just define the location based on its levels of continuous variables relevant to a given situation? This goes back to my comment above about the very binary nature of this approach. I am not yet convinced that this is really moving us forward a great deal. Though I am keeping an open mind as I read.

Response: As mentioned in L160 response, the location in time and space may be unknown. Equation (3) is related to spatial variability and uncertainty in site characterization, which leads to uncertainty in identifying the locations critical for HSHMs. The definition is needed to define the corresponding statistical random variables.

L225: I like the statistical framework here, though it presumes that we have complete (or very good) knowledge of the spatial and temporal factors governing HSHM 'activation' and I wonder if that makes this framework difficult to use? That is, if we already know the conditions that lead to HSHM behavior, then we already know that, and I am not clear on what we are learning from this framework.

Response: We agree with the reviewer that work in the HSHM community thus far has been remarkably site-specific. To enable the transferability of HSHM features from one site to the other, we have proposed this statistical framework. For example, static indicators at riparian sites could be quite similar – riparian buffer strips or microtopographic depressions. By using a statistical formulation to capture these spatial zones and applying them to a new site under corresponding dynamic conditions can help us pre-identify potential zones of HSHMs. It is also important to note that the impact of HSHMs does not depend only on the fact that they may exist in a certain compartment, i.e. riparian and hyporheic zones, but also on their location and duration in the active state, which may be intermittent. All these factors are uncertain because we don't know the exact location of HS and for how long they are active under new conditions and new sites. Thus, our stochastic approach is beneficial to enhance applicability to other sites. We have better demonstrated the key advantages of the approach in the revised manuscript (L54-L66, L226-L244, L506-L521).

L265: Again I am not understanding what we are learning here. The hot spots have been defined as NRZ with specific quantitative conditions. So what more is equation 10 telling us? I was expecting to see a figure or analysis here that went to the next level of understanding through the use of eq. 10.

Response: Equation 10 is an example how we can construct a static indicator quantitatively. Please also see our responses to L225 comment.

L340: Unless I am missing something, the examples are based around meeting specific conditions in space and/or time, and saying that if all conditions are met, then a HSHM should occur. That's all fine, but again, what are learning from that? It seems like this boils down to an if-else statement that is built around previous analyses of a given system. That seems really straightforward to the point that I fell like I am missing something. Maybe more of the implications can be drawn out through these sections?

Response: There is a challenge in knowing what the conditions required to trigger HSHMs are, but knowing the conditions may not suffice to predict when and where. This is where our proposed approach comes in. As mentioned above, our proposed framework is unified and allows us to investigate a variety of HSHMs, with complex dynamics multi-dimensional dynamics and under diverse conditions of uncertainty. It also can be easily integrated with the concept of Bayesian conditioning in order to reduce uncertainty and to develop site investigation schemes with information from similar sites. We do not promulgate an if-else approach, because we assign probabilities over the entire domain. The proposed equations and formula in this section are mainly presented to show how the framework can be utilized and how the corresponding indicators can be constructed.

Section 4.2.3: To be honest, I am not savvy enough to follow the math in this section. I can only assume that it is correct, and maybe other reviewers can go through it. Regardless of whether it is correct or not, however, I do not understand the purpose of the formulations. Maybe they come clear further into the paper. At this point this section and the previous two seem esoteric, and I am not sure what the work is really driving towards.

Response: In previous sections we focused on evaluating the probability of HSHMs occurring at a given time t. This allows us to evaluate when and where we could observe the highest probability of HSHM occur. As hot moments can persist over time periods, estimating the corresponding probabilities for given time intervals becomes also quite important. And this is the main reason for introduced section 4.2.3. In the revised manuscript, we have moved this section to the Appendix to balance mathematical deviation and discussion.

Specifically, Equation (22) – (26) describes the dynamic indicator and an analytical stochastic solution for the HSHM. These equations can be simplified into Equation (27) – (30) if the hot spot can be defined by a simple geometry as described in Line 458. The deviations of these equations are based on stochastic theories, which are well documented and extensively verified cf., Dagan. (1989) and Rubin. (2003).

Section 4.3: Not clear on what 'w' is in this case. More generally, I continue to struggle to understand what we are learning. I really want to get on board and I feel strongly about HSHMs as important features, I just am struggling to connect the conceptual dots.

Response: In most world conditions, HSHMs occur within a volume rather than a single spot. And this is why we introduced 'w' in the mathematical formulations, which represents the corresponding dimensions of this control volume (L422). We have also better defined $\boldsymbol{\Omega}^*$, t^* and the indicator random variable in L105-L108.

L515: Can you show a figure of this? pretty hard to understand as is.

Response: Hot spot Ω was placed $21I_{YH}$ away from the source, and the dimension of Ω is $(2I_{YH}, 2I_{YH}, 2I_{YV})$. Figure 3 presents the configuration of this example, where the red box is the candidate hot spot Ω.

L520-540: Okay, so now we start to see some results from the framework, in which the time course of HSHM development is linked to variation in conductivity. This is nice, though I must wonder whether the formal statistical framework is necessary. Could this be done just as well with a Monte Carlo approach? What I am missing is a convincing argument that the formal framework is needed. Could one not just run a simulation and sample it to characterize the spatial distribution of biogeochemical rates, use that to determine the frequency and magnitude of hot spots and then do that through time to show the time course?

Response: Our approach can definitely be applied using Monte-Carlo (MC) approaches. We present a framework, and it can be applied using analytical models (when available) or using MC simulation. These approaches are complementary rather than exclusive. One can use our framework to define the flowchart for the Monte-Carlo analysis. Although MC approach can be used for implementation, our approach goes further than MC because it can easily incorporate Bayesian concepts such as conditioning as well as utilization of prior information from other sites. For example, knowledge from previous nitrogen HSHM studies can be implemented with the proposed framework and guide new HSHM investigation at other new sites (L219-L225). Additional benefits are presented in L226-L244.

L595: I don't recall seeing any results showing how the framework can be used to study uncertainty. This seems important, but not presented.

Response: As we stated in point 1 and 6 above, our proposed framework incorporate uncertainty through modeling the dynamics as stochastic processes and through modeling the parameters as random variables. For example, in Section 4.4 (section 4.3 in revised manuscript), we show how the uncertainty surrounding the hydraulic conductivity influences the probability of HSHM occurrence in the subsurface.

L605: I think it would be useful to expand on the discussion through the manuscript in terms of how the framework provides understanding of mechanisms. Through much the paper it seemed that the mechanisms were known a priori and were actually used to define conditions that result in HSHMs. I don't fully understand how we are gaining more mechanistic understanding, but I am open to hearing more.

Response: We appreciate this comment. In the revised manuscript, we have incorporated certain Bayesian statistics theories into the indicator formulation and expanded the discussion correspondingly. The wide range of approaches used for modeling HSHMs reported in the literature are helpful in gaining a better understanding of HSHMs, however it is challenging to evaluate and rank the suitability of the models for realistic scenarios. This is where our study becomes useful. The flexibility of our proposed framework enables us to compare the performance of competing models and select appropriate models for new sites. And we would cite here a couple of examples. First, Bayesian model averaging approaches (Volinsky et al., 1999) could be implemented to obtain a combined and less risky estimation of HSHMs at new sites. Second, model comparison criteria, such as the Akaike information criteria (AIC, Akaike, 1974) and Bayesian information criteria (Schwarz, 1978) can also be applied to compare and rank the performance of different HSHM indicator models and their ability to explain observations. For example, smaller AIC and BIC values indicate a better match between a HSHM model and data. Large AIC and BIC values would suggest an incomplete and possibly even faulty model. Through this process of model inter-comparison, we could gain better understanding of the underlying mechanism, which, in essence, is the learning process that the reviewer rightfully wishes us to show. These modifications are reflected in L226-L244.

Statistical Characterization of Environmental Hot Spots and Hot Moments and Applications in Groundwater Hydrology

Jiancong Chen[1], Bhavna Arora[2], Alberto Bellin[3] and Yoram Rubin[1]

[1]Department of Civil and Environmental Engineering, University of California, Berkeley, California, USA
[2]Energy Geosciences Division, Lawrence Berkeley National Laboratory, Berkeley, California, USA
[3]Department of Civil, Environmental and Mechanical Engineering, University of Trento, Italy

Correspondence to: Yoram Rubin (rubin@ce.berkeley.edu)

Abstract

Environmental hot spots and hot moments (HSHMs) represent rare locations and events that exert disproportionate influence over the environment. While several mechanistic models have been used to characterize HSHMs behavior at specific sites, a critical missing component of research on HSHMs has been the development of clear, conventional statistical models. In this paper, we introduced a novel stochastic framework for analyzing HSHMs and the uncertainties. This framework can easily incorporate heterogeneous features in the spatiotemporal domain and can offer inexpensive solutions for testing future scenarios. The proposed approach utilizes indicator random variables (RVs) to construct a statistical model for HSHMs. The HSHMs indicator RVs are comprised of spatial and temporal components, which can be used to represent the unique characteristics of HSHMs. We identified three categories of HSHMs and demonstrated how our statistical framework are adjusted for each category. The three categories are (1) HSHMs defined only by spatial (static) components, (2) HSHMs defined by both spatial and temporal (dynamic) components, and (3) HSHMs defined by multiple dynamic components. The representation of an HSHM through its spatial and temporal components allows researchers to relate the HSHM's uncertainty to the uncertainty of its components. We illustrated the proposed statistical framework through several HSHM case studies covering a variety of surface, subsurface, and coupled systems.

1 Introduction

Environmental hot spots and hot moments (HSHMs) were originally defined as rare locations or events that support or induce disproportionately high activity levels (e.g., chemical reaction rates) compared to surrounding areas or preceding times (McClain et al., 2003). Vidon et al. (2010) further classified HSHMs into either transport-driven or biogeochemically-driven HSHMs, based on the mechanisms causing the HSHMs. Bernhardt et al. (2017) derived the concept of ecological control points (CPs) related to HSHMs, defining CPs as areas of the landscape that exert a disproportionate influence on the biogeochemical behavior of an ecosystem under study. These definitions have mainly focused on HSHMs related to elevated biogeochemical activities triggered by hydrological or biogeochemical processes, or a confluence of both processes. The concept of HSHMs is also used in climate science, where it is related to elevated greenhouse gas emissions or specific locations that are subject to extreme natural hazards (e.g., sea-level rise, floods, hurricanes, or earthquakes) caused by climate change ~~(Arora et al., 2020; Shrestha and Wang, 2018).~~(Arora et al., 2021; Shrestha and Wang, 2018). Further, Henri et al. (2015) related HSHMs to locations

experiencing elevated environmental risks and developed the incremental lifetime cancer risk (ILCR) model to quantify the effects of hot spots on human health. ~~Overall, these studies have focused on quantifying the consequences of HSHMs by way of environmental risks and costs while also emphasizing the importance of characterizing the occurrences of environmental HSHMs.~~ In the present study, we ~~combined these definitions~~ provide a unified treatment of both positive and negative impacts of HSHMs such that, ~~henceforth,~~ HSHMs are referred to as rare locations or events that could exert a disproportionate beneficial or destructive influence on an ecosystem ~~and~~, which ~~are associated with heightened health or environmental risks~~allows us to present an integrative analytical framework for understanding and modeling HSHMs in various fields.

~~Characterizing HSHMs dynamics is useful for understanding hydrological and ecological dynamics related to nutrient cycling, contaminant transport, and accurate assessment of ecosystem and hydrological perturbations under climate change. For example, Duncan et al. (2013) demonstrated that riparian hollows, which represent less than 1.0% of the landscape but contribute to more than 99% of total denitrification of a whole catchment area, function as hot spots. Additionally, wetlands have been considered biogeochemical hot spots for mercury mobilization and methylation production since the early 1990s (Vidon et al., 2010). The spatial patterns of methylmercury (MeHg) hot spots in wetlands can vary significantly across space. Indeed, the MeHg concentration at the interface between upland and peatland can be 100 times greater than a different patch within the same wetland (Mitchell et al., 2008). In managed temperate peatlands, drainage ditches that account for less than 5% of a land area can act as hot spots and can contribute to over 84% of total greenhouse gas emissions (Teh et al., 2011). The disproportionate contributions from HSHMs to the overall hydrological and ecological dynamics strongly indicate the necessities of characterizing HSHMs.~~

~~Quantifying HSHMs has also been recognized as important for assessing the consequences after catastrophes and the environmental risks, such as water crises (Baum et al., 2016) or nuclear disasters (Kamidaira et al., 2018; Morino et al., 2011; Showstack, 2014). The migration of contaminants after a catastrophe creates zones of different toxicity levels and poses disproportionate threats to the surrounding natural and urban environment. In contrast, existing HSHMs caused by the leakage of nuclear waste or heavy metals largely influence site characterization needs and the remediation efforts needed to minimize environmental and economic losses (Bao et al., 2014; Harken et al., 2019). Thus far, studies in this area have focused on the environmental implications and usefulness of characterizing HSHMs. However, special tools for characterizing and modeling HSHMs are still needed, such as physically based and statistical models, which can provide additional benefits to capture the disproportionate effects of an HSHM on a whole ecosystem.~~

~~Reactive transport models have been used to understand and predict HSHMs. Dwivedi et al. (2017), for instance, developed a 3-D high-resolution numerical model to investigate whether organic carbon-rich and chemically reduced sediments located within the riparian zone act as denitrification hot spots. Their study demonstrated a significantly higher potential (~70%) of the naturally reduced zones (NRZs) to remove nitrate than the non-NRZ locations. Arora et al. (2016) used a 2-D transect model and showed that temperature fluctuations constituted carbon hot moments in a contaminated floodplain aquifer that resulted in a 170% increase in annual groundwater carbon fluxes. Gu et al. (2012) developed a Monte Carlo reactive transport approach and discovered how~~

denitrification HSHMs are triggered by river stage fluctuations. Despite these studies, clear statistical conventions of HSHMs are missing, which significantly limits the transferability of these approaches. In fact, distinguishing HSHMs based on statistical formulations has been identified as a major gap in the current HSHM literature (Bernhardt et al., 2017; Arora et al., 2020).

Statistical approaches offer multiple advantages for furthering the HSHM concept. First, statistical approaches can develop common formulations that integrate biogeochemical and hydrogeological knowledge from multiple HSHMs studies. Once developed, these formulations can be readily applied to identify HSHMs at similar sites. Second, statistical approaches can easily incorporate categorical indicators that represent spatial heterogeneity and quantify the uncertainty of HSHM occurrences tied to these features. Such approaches can be used as predictive tools to estimate future occurrences of HSHMs, and provide an alternative to computationally expensive high-resolution mechanistic models. This would greatly aid decision makers in identifying scenarios (e.g., changes in the climate or in environmental conditions) that increase risks associated with the occurrence of HSHMs phenomena.

Statistical concepts and models have been widely applied in hydrology and hydrogeology, including but not limited to modeling flow and contaminant transport, quantifying subsurface heterogeneity and the associated uncertainties, developing strategies for site characterization, and providing informative priors for ungauged watersheds. For example, Rubin (1991) described a Lagrangian approach to obtain the spatial and temporal moments of contaminant concentrations in the subsurface. These statistical moments were deemed both necessary and sufficient to define the probability distribution of contaminant concentrations over space and time, and thus, quite useful for quantifying HSHMs. In a similar manner, statistical moments can be used to characterize the occurrences of HSHMs. Statistical terms, such as concentration mean and variance, concentration cumulative density function (CDF), exceedance probabilities, and exposure time CDF also provide significant guidance to assess the environmental risks associated with HSHMs (Rubin et al., 1994). Although there is a lack of conventional statistical approaches in current HSHM studies, we believe it is feasible and valuable to develop statistical formulations to characterize HSHMs dynamics.

Successful characterization of HSHMs through physically based models or statistical approaches relies on experts' knowledge of a site, intensive field characterization, and possibly continuous field sampling to provide the data to develop and validate these approaches. Understandably, intensive site characterization and long-term sampling can be quite challenging due to the associated costs and efforts. Thus, it is necessary to develop approaches that could simplify but still effectively and efficiently represent the underlying structure of HSHMs. In this regard, indicator statistics, defined by the Bernoulli distribution, can be useful, on two counts. First, it is suitable for modeling bimodal situations. For example, a situation where an event might or might not take place. Indicators are also appealing in applications because of the sparsity of the Bernoulli probability model. Indicator statistics have previously been applied to model flow and transport phenomena in groundwater (Rubin and Journel, 1991), where indicators were used to model the spatial distribution in a sand shale formation. Rubin (1995) applied an indicator spatial random function to model contaminant flow and transport in bimodal heterogeneous formations. Ritzi et al. (2004) developed a hierarchical architecture to represent the spatial correlation of permeability in cross stratified sediment using indicator statistics. Wilson and Rubin (2002) and Bellin and Rubin (2004) used indicator statistics that describe

~~whether particles were captured by sampling points to characterize the level of aquifer heterogeneity. These studies suggest that the simplification of the system's structure through indicator formulation significantly lower the number of measurements needed, and thus reduce the costs associated with site characterization, while maintain sufficient information for modeling flow and contaminant transport. In addition, indicator formulation is useful in that it allows to aggregate multiple variables (e.g., all HSHM relevant variables) into a single random variable. Instead of characterizing the full distributions of each parameter, indicator formulation only requires knowledge of the critical condition for relevant parameters. Such indicator RV will take a value of 1 if the critical conditions are met, regardless of the original distribution for the parameters. These advantages are further explored in section 2 and 3. With indicator formulations for HSHMs, researchers can focus on identifying the most relevant parameters for HSHMs quantification, which can significantly reduce the efforts and costs required for intensive site characterization.~~

~~In this study, we developed a statistical framework to quantify HSHMs occurrences and uncertainties. The developed statistical framework can help determine HSHM occurrence probabilities under user-defined scenarios. It can also be used for estimating future occurrences of HSHMs. Based on the mechanisms that drive HSHM occurrences, we determined~~Various approaches have been developed to better quantify HSHMs dynamics, including numerical modeling, empirical modeling and data-based approaches with statistics. For example, Dwivedi et al. (2017) developed a 3-D high-resolution numerical model to investigate whether organic-carbon-rich and chemically-reduced sediments located within the riparian zone act as denitrification hot spots. Their study demonstrated a significantly higher potential (~70%) of the naturally reduced zones (NRZs) to remove nitrate than the non-NRZ locations. Arora et al. (2016b) used a 2-D transect model and showed that temperature fluctuations constituted carbon hot moments in a contaminated floodplain aquifer that resulted in a 170% increase in annual groundwater carbon fluxes. Gu et al. (2012) developed a Monte Carlo reactive transport approach and discovered how denitrification HSHMs are triggered by river stage fluctuations. Abbott et al. (2016) developed the HotDam frameweork that combines the HSHM concept and Darmköhler number with multiple tracers to advance our understanding of ecohydrology. Statistical concepts have also been used to identify HSHMs through simple comparison to average or matrix; substantial percentage of total flux; outlier in distribution of data; statistically significiant difference between or among landsape elements and contribution to flux/total area or time (Bernhardt et al. (2017) and references therein). Wavelet and entropy-based approaches have also been used to identify non-uniform regions and times and consequently HSHMs (Arora et al., 2013, 2019a). However, most of these quantitative methods are derived based on site-specific data, which severely limits the transferability of these approaches. In contrast, a unified HSHM approach offers multiple advantages. First, a unified strategy based on commonly-used parameters for a given HSHM would allow modelers to create probability priors that could be used for prediction of said HSHM at unnsampled- or poorly-sampled sites (Li et al., 2018). Second, such a standardized approach for modeling HSHMs could be beneficial to developing and implementing monitoring standards and regulations for environmentally-senstive HSHMs. Last, but not the least, a unified approach can be used together with mechanistic models to capture uncertaintiy and heterogeneity for HSHMs in environmentally-relevant applications.

Successful characterization of HSHMs through deterministic physically-based models or purely statistical approaches relies on experts' knowledge of a site, intensive field characterization, and possibly continuous field

sampling to provide the data to develop and validate these approaches. Understandably, intensive site characterization and long-term sampling can be quite challenging due to the associated costs and efforts. In this regard, having access to a stochastic approach that could improve predictions through built-in model updating (i.e., Bayesian) capabilities could prove to be an advantage.

Stochastic concepts and models have been widely applied in hydrology and hydrogeology for addressing situations subject to uncertainty, including but not limited to modeling flow and contaminant transport, quantifying subsurface heterogeneity and the associated uncertainties, developing strategies for site characterization, and providing informative priors for ungauged watersheds. Bayesian approaches were found particularly useful, especially through the conceprts such as conditioning and updating. In this paper, we aim to bring the experience gained in hydrology and hydrogeology into HSHM modeling.

An important characteristic of HSHMs is that they occupy a limited portion of the investigated domain and may be active for a limited amount of time since they are activated when the control variable exceeds a given threshold. Physical and geochemical heterogeneities, and the impossibility to fully characterize them, render the deterministic identification of HSHMs a vanishing objective. To address the hurdle, we propose to cast the problem into a probabilistic framework by seeking the probability of HSHM occurrence at a given position and time. For a given time and/or space intervals and for a-priori specified HSHM criteria, an HSHM occurrence could be viewed as a binary variable where the ensemble mean is the probability of occurrence. Indicator statistics have previously been applied to model flow and transport phenomena in groundwater (Rubin and Journel, 1991), where indicators were used to model the spatial distribution in a sand-shale formation. Wilson and Rubin (2002) and Bellin and Rubin (2004) used indicator statistics to characterize aquifer heterogeneity. These studies suggest that representation of a system's structure through indicator formulation holds the potential of taking informed decisions, for example concerning remediation actions, under incomplete site characterization.

Based on the mechanisms that trigger HSHMs, we identified three categories of HSHMs: (1) those triggered only by spatial (static) contributors, (2) those triggered by both spatial (static) and temporal (dynamic) contributors, and (3) those triggered by multiple dynamic contributors. ~~Within each category, cases from existing studies were used to illustrate the procedures for constructing the statistical formulations. We focused specifically on HSHMs applications in groundwater, where we derived analytical solutions for the statistical formulation of HSHMs and analyzed the probabilities of HSHM occurrences and their corresponding levels of uncertainty using synthetic case studies~~Applications of the proposed indicator formulation to a diverse range of HSHM situations are presented to illustrate the generality of our proposed approach. The remainder of the paper is structured as follows. Section 2 outlines the proposed statistical framework for predicting HSHMs. In section 3, various reported cases from previous HSHM studies are presented using the framework of our proposed approach, intended to demonstrate its generality. In section 4, we present an HSHM application in groundwater hydrology and show how the HSHM uncertainty relates to the spatial variability of the hydraulic conductivity. Advantages and limitations of our approach are discussed in section 5.

2 ~~Statistical~~Methodology and statistical formulation of HSHMs

Herein, we present a statistical formulation of hot spots and hot moments, which considers the HSHM occurrence as a binary event, expressed through indicator statistics embedded with the HSHM underlying physics. Section 2.1 summarizes the indicator formulation of HSHMs. Based on the contributors to HSHMs, we classified HSHMs into three different types, and we demonstrate how indicators are constructed for each type of HSHM in sections 2.2, 2.3 and 2.4, respectively. Section 2.5 focuses on the linkages between indicators and Bayesian concepts. Case studies for each class of HSHMs are provided in Section 3.

2.1 Indicator formulation of HSHMs

HSHMs represent ~~rare places~~ intervals in space and/or ~~events with increased~~time characterized by hydrobiogeochemical activity rates or fluxes that ~~are~~differ significantly ~~elevated above~~from the background ~~condition~~conditions, thus exerting disproportionate influences over an ecosystem's dynamics. We define ~~$(\boldsymbol{\Omega}^*, t^*)$~~ $\boldsymbol{\Omega}^*$ as the volume (subdomain) within which the hot spot is verified and ~~t^*) as the jointly distributed RVs for HSHMs, and $\boldsymbol{\Omega}^*$ and t^* represent the spatial components of hot spots and temporal components of~~ the time at which the hot ~~moments, respectively.~~ moment occurs. An indicator random variable, $I_{HSHM}(\boldsymbol{\Omega}^*, t^*)$, is used to ~~represent~~identify whether ~~the pair~~HSHM occurs at $(\boldsymbol{\Omega}^*, t^*)$ ~~is an HSHM~~ or not. If ~~there exists a pair of $(\boldsymbol{\Omega}^*, t^*)$ that satisfies the~~ user-defined critical conditions ~~of~~needed to trigger an HSHM~~,~~ are met at $(\boldsymbol{\Omega}^*, t^*)$, then $I_{HSHM}(\boldsymbol{\Omega}^*, t^*) = 1$, and it is equal to zero otherwise. What makes the indicator a random variable is the uncertainty in the ~~pair $(\boldsymbol{\Omega}^*, t^*)$ represents the location~~spatial and ~~time of~~temporal distribution of the quantities triggering the HSHM~~.~~ event in real-life applications. Following the original definition by McClain et al. (2003), in our method, $I_{HSHM}(\boldsymbol{\Omega}^*, t^*)$ can take the value of 0 or 1, depending on ~~the concentration or reaction rate measure at $(\boldsymbol{\Omega}^*, t^*)$, respectively~~whether suitable thresholds are exceeded or not as follows:

$$I_{HSHM}(\boldsymbol{\Omega}^*, t^*) = \begin{cases} 1, if\ C(\boldsymbol{x}, t^*) > C_{th};\ \boldsymbol{x} \subseteq \boldsymbol{\Omega}^* \\ 0, \qquad otherwise \end{cases}, \text{ or}$$

$$I_{HSHM}(\boldsymbol{\Omega}^*, t^*) = \begin{cases} 1, if\ R(\boldsymbol{x}, t^*) > R_{th};\ \boldsymbol{x} \subseteq \boldsymbol{\Omega}^* \\ 0, \qquad otherwise \end{cases}, \quad (1)$$

where $C(\boldsymbol{x}, t^*)\ and\ R(\boldsymbol{x}, t^*)$ are the concentration and reaction rate at the position $\boldsymbol{x}$ and time t^*, respectively. $C_{th}\ and\ R_{th}$ represent the concentration and reaction rate thresholds, respectively~~,~~ which identify whether HSHM is triggered or not. Defining indicators with concentration~~,~~ or reaction rate depends on the target of HSHM. ~~Similar definitions~~The threshold values can also be ~~introduced~~ based on ~~the~~ regulatory limits or ~~the interest of the investigator, using the mean concentration or the solute mass within the volume $\boldsymbol{\Omega}^*$.~~defined by the user.

The critical values~~,~~ of C_{th} and/or R_{th}~~,~~ are ~~key~~keys to an effective application of the above framework and should be determined based on the specific scenario~~.~~ under investigation. For example, ~~for~~in the case of contaminants that are associated with significant environmental or health risks (e.g., nuclear waste or a cancerous substance), $C_{th} = 0$ or $R_{th} = 0$ can be used so that the HSHM will be triggered as soon as there is the presence of such contaminants~~.~~ and relevant chemical reactions. As an alternative, a limit in the total accumulated mass or fluxes within hot spots may also be set, such as suggested by EPA (USEPA, 2001), but in this case the definition (1) of the indicators should be modified. For water quality parameters, $C_{th} = MCL$ or $R_{th} = R^*$ can be assigned, where MCL represents the maximum

concentration limit for a specific solute~~.~~ whereas R^* could represent a critical reaction rate. The critical thresholds can be determined based on statistics, such as percentiles and extremes as defined by regulations or analytical studies. Alternatively, C_{th} ~~$= C^*$ can be used in cases where C^* is~~ and R_{th} could also be chosen based on the experts' domain knowledge~~. This~~ or from well-documented studies at similar environments. Through the flexibility to adopt different choices for activation thresholds, our approach ~~requires that such decisions be made before deriving any solutions to determine~~could allow users to compare relevant indicator models and assess their applicability by testing how different thresholds would influence the probability of the HSHM ~~occurrences~~to occur and assessing said probabilities against risk tolerance and/or regulations.

~~Given~~Following the definition of $I_{HSHM}(\boldsymbol{\Omega}^*, t^*)$~~,~~ as a binary random variable (Eq. 1), we ~~observe that $I_{HSHM}(\boldsymbol{\Omega}^*, t^*)$ follows~~propose to model it with a Bernoulli distribution, such as~~–~~ $I_{HSHM}(\boldsymbol{\Omega}^*, t^*) \sim Bernoulli(< I_{HSHM}(\boldsymbol{\Omega}^*, t^*) >)$, where $< . >$ is the ~~operator indicating the~~ ensemble ~~mean of the indicator represented as a random variable~~averaging operator. An important characteristic of the Bernoulli distribution is that all the statistical moments of the RV $I_{HSHM}(\boldsymbol{\Omega}^*, t^*)$ can be expressed as a function of the ensemble mean $< I_{HSHM}(\boldsymbol{\Omega}^*, t^*) >$. For example, the variance is given by $var\left(I_{HSHM}(\boldsymbol{\Omega}^*, t^*)\right) = < I_{HSHM}(\boldsymbol{\Omega}^*, t^*) > \cdot (1 - < I_{HSHM}(\boldsymbol{\Omega}^*, t^*) >)$. Thus, being able to fold the HSHM physics into an indicator formulation, a simplified approach is presented through Eq. (1).

~~Characterization~~Case-based formulation of the ~~spatiotemporal~~Bernoulli distribution of $I_{HSHM}(\boldsymbol{\Omega}^*, t^*)$ requires the incorporation of the mechanisms that govern the development and occurrence of HSHMs~~. However, the direct quantification of $< I_{HSHM}(\boldsymbol{\Omega}^*, t^*) >$ can be difficult in both time and space domain. Thus, to~~ into the indicator model. To facilitate this undertaking, we propose to decompose $I_{HSHM}(\boldsymbol{\Omega}^*, t^*)$ into a Type-A (static) indicator random variable~~ $I_s, I_s(\boldsymbol{\Omega}^*)$),~~ and a Type-B (dynamic) indicator random variable~~ $I_d, I_d(\boldsymbol{\Omega}^*, t^*)$~~. Definitions of the Type-A and Type-B ~~contributors~~indicators are ~~as follows~~provided herein:

- **Type-A (Static) Contributors.** This category covers discrete spatial elements (and their associated critical states) that could trigger an HSHM once they come into contact with Type-B contributors (see discussion below). Critical states are the range of values needed to trigger an HSHM (either in standalone mode or when coupled with Type-B contributors).
- **Type-B (Dynamic) Contributors**. This category covers dynamic variables (and their associated critical states) that could trigger an HSHM once they come into contact with Type-A contributors. This category includes, for example, mass transport variables. It also includes changes in local hydrological and environmental conditions (e.g., water table fluctuations). The displacement of solutes in the subsurface (trajectories and travel times) from below- and above-ground processes are prime examples of Type-B contributors.

As an example, naturally reduced sediments (Type-A contributor) occurring next to the river corridor at the Rifle site were identified as carbon export hot spots ~~(Arora et al., 2016; Wainwright et al., 2015)~~(Arora et al., 2016a; Wainwright et al., 2015). Studies showed that these hot spots were triggered when temperature conditions (Type-B contributor) varied in the subsurface, resulting in a 170% increase in groundwater carbon export from the floodplain site to the river ~~(Arora et al., 2016).~~(Arora et al., 2016b). In another example, topographic features, such as the

backslope of the lower montane hillslope (Type-A contributor) within the East River Watershed (Hubbard et al., 2018), were considered denitrification hot spots, which can have a significant impact on the watershed-scale nitrogen loss pathway. These hot spots were often triggered by spring snowmelt and storm events (Type-B contributor).

Both indicators of the ~~Type~~type-A and ~~Type~~type-B contributors assume a value of either 0 or 1. If one of these indicators takes a value of 1, it can be viewed as an HSHM contributor. However, for an HSHM to occur, both indicators must have a value of 1 at the same location and time. This idea can be expressed as follows:

$$P(I_{HSHM}(\boldsymbol{\Omega}^*, t^*) = 1) = P(I_s(\boldsymbol{\Omega}^*) = 1, I_d(\boldsymbol{\Omega}^*, t^*) = 1)$$
$$= P(I_s(\boldsymbol{\Omega}^*) = 1) \cdot P(I_d(\boldsymbol{\Omega}^*, t^*) = 1 | I_s(\boldsymbol{\Omega}^*) = 1)$$
$$= P(I_d(\boldsymbol{\Omega}^*, t^*) = 1) \cdot P(I_s(\boldsymbol{\Omega}^*) = 1 | I_d(\boldsymbol{\Omega}^*, t^*) = 1). \quad (2)$$

~~In Eq. (2), $P(I_d(\boldsymbol{\Omega}^*, t^*) = 1 | I_s(\boldsymbol{\Omega}^*) = 1)$ is the probability of observing a dynamic HSHM within $\boldsymbol{\Omega}^*$, at time t^* conditional to the fact that $\boldsymbol{\Omega}^*$ is a static hotspot and $P(I_s(\boldsymbol{\Omega}^*) = 1 | I_d(\boldsymbol{\Omega}^*, t^*) = 1)$ is defined similarly. Based on the mechanisms of HSHMs, we can classify HSHMs into three different categories as discussed below. These categories can be used to guide the application of the above statistical framework in a variety of complex HSHM scenarios, and they can also be used to develop analytical or numerical solutions for both static and dynamic indicators. Furthermore, the three categories provide guidance on using indicator approaches for both transport driven and biogeochemically driven HSHMs, as discussed by Vidon et al. (2010).~~

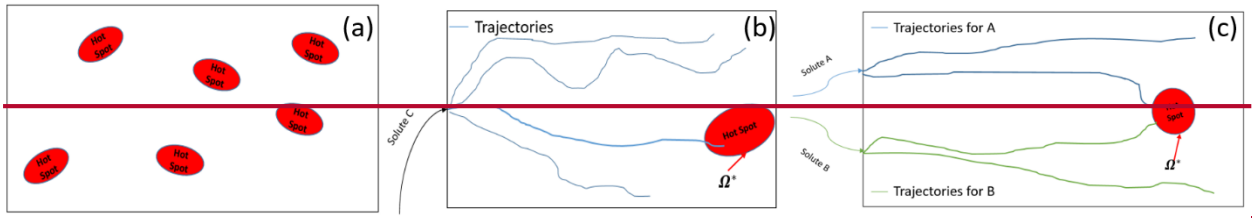

~~Figure 1. Identified categories of HSHMs.~~ Based on the mechanisms of HSHMs, we can distinguish between three different HSHM categories as discussed below. These categories can be used to guide the application of the above statistical framework in a variety of complex HSHM scenarios, and they can also be used to develop analytical or numerical solutions for both type-A and type-B contributors.

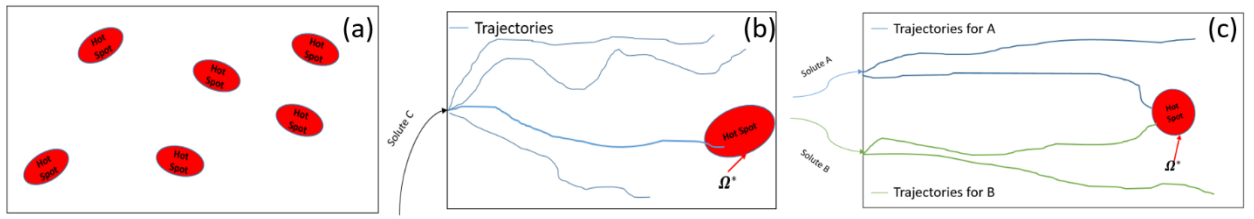

Figure 1. Identified categories of HSHMs. Panel (a) presents HSHMs resulting from ~~only~~ Type-A (static) indicator only; panel (b) presents HSHMs resulting from coupled action (static + dynamic) and panel (c) presents HSHMs resulting from multiple (two) dynamic indicators.

2.~~1~~2 HSHMs induced by type-A (static) indicators

In this section, we consider HSHMs that are defined by static indicators only (Figure 1a). This list can include zones of high, persistent concentration and reactivity that are due to the subsurface or the ecosystem's unique hydrological and biogeochemical properties. For example, the accumulation of contaminants in the subsurface (e.g.,

the high nuclide concentration in the subsurface at the Hanford site) could lead to the evolution of persistent, high reactivity zones. An aquifer's reactivity is another example that could distinguish certain regions with high reactivity compared to surrounding areas (Loschko et al., 2016). Such high reactivity spots (hereafter denoted as $\boldsymbol{\Omega}^*$) can be characterized by static indicator RVs due to the persistence of high concentration or reactivity. The static indicators are defined as follows:

$$I_{HSHM}(\boldsymbol{\Omega}^*) = I_s(\boldsymbol{\Omega}^*) = \begin{cases} 1, & if\ Z(\boldsymbol{\Omega}^*) \subseteq Z_s^* \\ 0, & otherwise \end{cases}, \tag{3}$$

where $Z_s{}^*$ represents the conditions needed to trigger a hot spot at $\boldsymbol{\Omega}^*$, and $Z(\boldsymbol{\Omega}^*)$ represents the corresponding local conditions at $\boldsymbol{\Omega}^*$. Notice that $\boldsymbol{\Omega}^*$ is a volume centered at a selected position of the domain where the probability of developing HSHM is evaluated.

2.~~2~~3 HSHMs induced by type-A (static) and type-B (dynamic) indicators

HSHMs can also result from dynamic processes encountering specific local conditions at $\boldsymbol{\Omega}^*$ (Figure 1b). This is the situation described by Eq. (2), where the ~~static~~type-A indicators are determined first, and then used jointly with the ~~dynamic~~type-B indicators for complete HSHM characterization. For example, Bundt et al. (2001) concluded that locations ($\boldsymbol{\Omega}^*$) interested by preferential flow paths are possible biological hot spots for soil microbial activities. ~~Preferential flow paths in such cases are candidate hot spot locations ($\boldsymbol{\Omega}^*$).~~ Meanwhile, dynamic factors, such as snowmelt~~,~~ or rainfall infiltration control contaminant transport via the preferential flow paths~~,~~ and thus, ~~they determined~~constitute the hot moment component. ~~The duration of these events presents the temporal component of the HSHM~~Additional case studies are presented in Section 3.

For ~~an HSHM~~HSHMs induced by both ~~static~~type-A and ~~dynamic~~type-B indicators, the static locations are selected first, based on their HSHM-related properties. After this, we can focus on characterizing the HSHM dynamics as they relate to the relevant locations. A selected location, $\boldsymbol{\Omega}^*$, could become an HSHM site based on characteristics defined through the following ~~static~~type-A and ~~dynamic~~type-B indicators, respectively:

$$I_s(\boldsymbol{\Omega}^*) = \begin{cases} 1, & if\ Z_s(\boldsymbol{\Omega}^*) \subseteq Z_s^* \\ 0, & otherwise \end{cases}, \tag{4}$$

$$I_d(\boldsymbol{\Omega}^*, t^*) = \begin{cases} 1, & if\ Z_d(\boldsymbol{\Omega}^*, t^*) \subseteq Z_d^* \\ 0, & otherwise \end{cases}, \tag{5}$$

$$I_{HSHM}(\boldsymbol{\Omega}^*, t^*) = \begin{cases} 1, & if\ Z_s(\boldsymbol{\Omega}^*) \subseteq Z_s^*, and\ Z_d(\boldsymbol{\Omega}^*, t^*) \subseteq Z_d^* \\ 0, & otherwise \end{cases}, \tag{6}$$

where Z_d^* represents the critical conditions needed to ~~characterize a~~ trigger the hot moment, ~~and~~whereas $Z_d(\boldsymbol{\Omega}^*, t^*)$ represents the corresponding, critical-state local ~~condition~~conditions at t^* and $\boldsymbol{\Omega}^*$. The statistical model of $I_{HSHM}(\boldsymbol{\Omega}^*, t^*)$ can be expressed using the statistical models of I_s and I_d, as shown in Eq. (2).

2.~~3~~4 HSHMs induced by multiple type-B (dynamic~~)~~) indicators

~~Various~~A confluence of dynamic processes could ~~jointly evolve into an~~result in the formation of a HSHM (Figure 1c). Unlike the previous scenarios where static locations can be determined through known characteristics provided by geophysical or other types of data, HSHMs can also emerge due to ~~the~~a confluence of dynamic processes. ~~This situation is described in Eq. (7).~~ For example, Gu et al. (2012) analyzed how streamflow fluctuations could trigger

a nitrogen HSHM. In their example, the dynamics of the streamflow and groundwater controlled the transport and mixing of the chemical reactants, thus triggering the occurrences of HSHMs. For this case, the static locations of $\boldsymbol{\Omega}^*$ are determined by the confluence of multiple dynamic processes~~.~~, not being restricted by a set of local conditions. In this case, only type-B indicators need to be modeled.

We can consider the case where an HSHM is predicated on m dynamic processes, d_j, where $I_{d,j}(\boldsymbol{\Omega}^*, t^*)$ is the dynamic ~~indicator representing the action (or inaction) of~~for each dynamic d_j at $\boldsymbol{\Omega}^*$ and time t^*. The hot spot location $\boldsymbol{\Omega}^*$ is determined by the confluence of all dynamic processes at time t^*. These dynamic processes are not necessarily independent. Therefore, generally, the statistical model for the comprehensive dynamic indicator (which covers all dynamic contributors) assumes the following form:

$$P[I_d(\boldsymbol{\Omega}^*, t^*) = 1] = P\left[I_{d,1}(\boldsymbol{\Omega}^*, t^*) = 1, \dots, I_{d,m}(\boldsymbol{\Omega}^*, t^*) = 1\right]. \quad (7)$$

In situations where the various dynamic contributors can be viewed as independent (e.g., ~~Destouni and Cvetkovic, 1991)~~ Destouni and Cvetkovic, 1991)—i.e., where the reactants travel via different paths—then, assuming independence, we can state that

$$P(I_d(\boldsymbol{\Omega}^*, t^*) = 1] = \prod_{j=1}^{m} P\left[I_{d,j}(\boldsymbol{\Omega}^*, t^*) = 1\right]. \quad (8)$$

Here, the mean of the dynamic indicator becomes

$$< I_d(\boldsymbol{\Omega}^*, t^*) > = \prod_{j=1}^{m} < I_{d,j}(\boldsymbol{\Omega}^*, t^*) >. \quad (9)$$

If $\boldsymbol{\Omega}^*$ is a hot spot, then Eq. (9) also defines $< I_{HSHM}(\boldsymbol{\Omega}^*, t^*) >$. However, if $\boldsymbol{\Omega}^*$ is not a hot spot, then we need to resort to coupled statistical modeling, as suggested by Eq. (2).

2.5 Additional advantages of stochastic formalism

The statistical framework also provides several benefits. Unified formulations of HSHMs through indicators provide us a platform to evaluate alternative HSHM models thoroughly and objectively. For example, the Akaike information criteria (AIC, Akaike, 1974) and Bayesian information criteria (Schwarz, 1978) can be used to rank between alternative indicator formulations and evaluae their ability to explain HSHM observations. Smaller AIC and BIC values indicate more information preserved in a given indicator HSHM model and implies better model quality than other indicator models. On the other hand, if larger AIC and BIC values are observed, important processes for HSHMs are likely missing indicating the necessity of increasing site characterization and refinement of conceptual models.

In addition, informative priors constructed from similar HSHM sites (Cucchi et al., 2019; Li et al., 2018) could advance early stage planning for HSHM site investigation. Knowledge from studies at similar HSHM sites can be summarized into prior distributions, which can account for variabilities within and between sites. For example, Cucchi et al. (2019) demonstrated how the distribution of hydraulic parameters at unknown target sites can be predicted using information from hydrologically similar sites with existing tool packages such as exPrior. Goal-oriented site characterization also becomes feasible with informative priors; for example, Li et al. (2018) demonstrated the usefulness of informative priors in reducing model uncertainty and potential risks for estimating groundwater

drawdown at Mintang tunnel in China. Therefore, through integration with statistical concepts, unified formulations of HSHMs enable us to integrate Bayesian concepts to obtain combined and less risky estimations of HSHMs at new sites, which can help us gain better understanding of the underlying mechanism.

3 Examples of the statistical formulation of HSHMs with case studies

In this section, we selected numerous examples from published research to present how our approach can be used to derive statistical representations for the HSHMs investigated in these studies. We grouped these studies into three categories based on the similarities of their underlying HSHM mechanisms, as described in section 2. ~~We also characterized~~Section 3.1 demonstrate the ~~environmental risk levels~~ formulation of static only HSHM; section 3.2 present the case with static and ~~impacts based on their target~~dynamic triggered HSHMs~~.~~ and section 3.3 summzerize the steps to construct multiple dynamic indicators for HSHMs. Table 1 presents a summary of these cases. ~~The indicator formulation is constructed in sections 3.1–3.3.~~where environmental risk levels as well as impacts on ecosystem were also included.

Reference	HS Location	Category	Seasonality	Environmental Risk	Causes	Impact	Static Mechanism	Dynamic Mechanism	HSHM Action	Metrics for threshold	Equation(s)
Examples of static only mechanisms											
Wainwright et al. (2015)	Naturally reducing zone	Subsurface	--	Short-term low risk; long-term high risk	Anthropogenic + Natural	Negative	Mineralological and lithological differences	--	Vanadium, uranium, metallic minerals	Concentration	(3)
Sassen et al. (2012)	Reactive facies	Subsurface	--	Short-term low risk; long-term high risk	Anthropogenic + Natural	Negative	Lithological differences	--	Uranium and other isotopes	Concentration	(3)
Examples of static + dynamic mechanism											
Andrews et al. (2011)	Shale hill	Subsurface + Surface	Snowmelt and fall flushing periods	Low risk	Natural	Neutral	South-facing concave hillslopes	Snowmelt and fall flushing periods	Organic carbon	Concentration	(4) – (6)
Henri et al. (2015)	Preferential flow path	Subsurface	--	High risk	Anthropogenic	Negative	Subsurface heterogeneity	Contaminant transport and travel time distribution	Chlorinated compounds	Concentration	(4) – (6)
~~Duncan et al. (2013)~~Duncan et al. (2013)	Microtopography	Surface	Unimportant	High risk	Natural	Positive	Riparian hollows	Transport and retention of reactants	Nitrogen	Concentration or reaction rate	(4) – (6)
~~Arora et al. (2016)~~Arora et al. (2016)	Naturally reducing zone-induced transport	Subsurface	Temperature and water table fluctuation	Low risk	Anthropogenic + Natural	Neutral	Naturally reduced zones	Temperature and water table fluctuation	Carbon fluxes	Concentration or reaction rate	(4) – (6)
Examples of multiple dynamic mechanisms											
Hill et al. (2000)	Riparian zone	Subsurface	--	High risk	Natural	Positive	Interfaces in the riparian zone	Supply of electron donor and acceptor from flow transport	Nitrogen and carbon	Concentration or reaction rate	(7) – (9)
Mitchell et al. (2008)	Peatlands	Subsurface + Surface	Summer periods	High risk	Natural	Negative	Upland-peatland interfaces induced by flow	Interactions between upland and peatland flow	Methylmercury	Concentration	(7) – (9)
Frei et al. (2012)	Microtopography	Surface	--	Neutral	Natural	Neutral	Flowpaths induced by microtopography	Biogeochemical evolution along flow paths	Organic matter and nitrogen	Concentration or reaction rate	(7) – (9)
Gu et al. (2012)	Mixing zones	Subsurface + Surface	River discharge + Water table fluctuation	High risk	Natural	Positive	Mixing zones caused by river stages	Interaction between surface water and groundwater	Nitrogen	Concentration or reaction rate	(7) – (9)

Table 1. Example cases considered in this study for constructing the statistical formulation of HSHM.

3.1 HSHMs triggered by static contributors only

In this section, we use Wainwright et al. (2015) as an example to illustrate our process to construct $I_{HSHM}(\boldsymbol{\Omega}^*, t^*)$ following Eq. (3), where an HSHM is triggered by static contributors only (section 2.1). NRZs within floodplain environments at the Rifle site are considered biogeochemical hot spots because they represent elevated concentrations of uranium, organic matter, and geochemically reduced minerals and they have been found to contribute to significant carbon fluxes to the atmosphere and to local rivers (Arora et al., 2016). Due to its characteristics, we considered the spatial distribution of an NRZ to be a static-mechanism-based hot spot. Wainwright et al. (2015) used geophysical data (e.g., induced polarization) to map the distribution of an NRZ at the subsurface level. They found that the phase shift (ϕ) from the induced polarization data of the NRZ was within $[4.5, 5] mrad$, compared to non-NRZ locations at $\phi \subseteq [1, 3.5] mrad$. Thus, ϕ can be used to construct the static indicator with a critical condition of $[4.5, 5] mrad$. Therefore,

$$I_s(\boldsymbol{\Omega}^*) = \begin{cases} 1, & if\ Z_\phi(\boldsymbol{\Omega}^*) \subseteq [4.5, 5]\ mrad \\ 0, & otherwise \end{cases}. \quad (10)$$

Other static attributes, including but not limited to elevation, hydraulic conductivity, and resistivity, can also be used to define the critical conditions to construct the static indicator for hot spots through Bayesian conditioning.

3.2 HSHMs occuring when dynamic contributors coincide at locations defined by static contributors

The second case we present here utilizes Eq. (4)–(6), where HSHMs are triggered when dynamic contributors coincide at hot spots determined by static contributors. Here, we present the case investigated by ~~Duncan et al. (2013)~~Duncan et al. (2013), where riparian hollows representing less than 1% of the total catchment area contributed to more than 99% of the total denitrification within the watershed. In their study, the denitrification rates peaked during the base flow (midsummer) period, when the riparian hollows were partially oxygenated and the hydrologic fluxes were at a minimum. The site was considered to have low inorganic N availability, and thus, nitrate was supplied via nitrification. The highest rates of denitrification were therefore tied to nitrification and the partially aerated conditions.

The static indicator needs to be constructed based on the microtopographical features within the riparian zone. Specifically, the topographic wetness index (TWI) ~~(Beven and Kirkby, 1979; Sørensen et al., 2006)~~(Beven and Kirkby, 1979; Sørensen et al., 2006) was used in Duncan et al. (2013) to delineate the riparian hollows from other riparian locations. Terrain analysis indicated a TWI threshold value of 6.0 and 8.0 for riparian hollows under wet and dry conditions, respectively, whereas 4.8 and smaller TWI values corresponded to other riparian locations (e.g., hummocks). Thus, the static indicator can be constructed using the TWI values within the riparian zone to determine the hot spot locations—the hollows. Hence,

$$I_s(\boldsymbol{\Omega}^*) = \begin{cases} 1, & if\ Z_{TWI}(\boldsymbol{\Omega}^*) > 6\ (wet\ condition)\ \text{or}\ 8\ (dry\ condition) \\ 0, & otherwise \end{cases}. \quad (11)$$

Multiple dynamic processes control the denitrification rate at the riparian hollows. As examined by ~~Duncan et al. (2013)~~Duncan et al. (2013), a partially aerated condition ($C_{O_2} > 5\%$) is needed to support nitrification, which supplies the nitrate for denitrification. As quiescent, non-storm periods during base flow favor the coupled nitrification-denitrification mechanism, this is another key process that needs to be represented by a dynamic indicator.

Although ~~Duncan et al. (2013)~~Duncan et al. (2013) did not mention specific concentration ranges for nitrogen species, the major components, such as organic N, should be available. Therefore, we can construct the dynamic indicators as follows:

$$P[I_d(\boldsymbol{\Omega}^*, t^*) = 1] = P\left[I_{d,O_2}(\boldsymbol{\Omega}^*, t^*) = 1, I_{d,Hydro}(\boldsymbol{\Omega}^*, t^*) = 1, I_{d,N}(\boldsymbol{\Omega}^*, t^*) = 1\right], \quad (12)$$

where $I_{d,Hydro}(\boldsymbol{\Omega}^*, t^*)$ is the dynamic indicator representing the streamflow stages; this will be 1 if the base flow conditions are met. Additionally, here, $I_{d,N}(\boldsymbol{\Omega}^*, t^*)$ is the dynamic indicator for the transport of the nitrogen species in the subsurface that support the coupled nitrification-denitrification mechanism.

$$I_{d,O_2}(\boldsymbol{\Omega}^*, t^*) = \begin{cases} 1, & if\ C_{O_2}(\boldsymbol{\Omega}^*, t^*) > 5\% \\ 0, & otherwise \end{cases},$$
$$I_{d,Hydro}(\boldsymbol{\Omega}^*, t^*) = \begin{cases} 1, & if\ t^* \subseteq base\ flow\ periods \\ 0, & otherwise \end{cases}, \quad (13)$$
$$I_{d,N}(\boldsymbol{\Omega}^*, t^*) = \begin{cases} 1, & if\ C_N(\boldsymbol{\Omega}^*, t^*) > 0 \\ 0, & otherwise \end{cases}.$$

It is noted that these dynamic processes are not statistically independent. Usually, when one condition is met (e.g., base flow conditions), other conditions may consistently be satisfied (e.g., the transport of nitrogen in riparian hollows). ~~Alternatively, numerical modeling approaches are more feasible to construct the dynamic indicators based on the critical conditions at riparian hollows ($\boldsymbol{\Omega}^*$), where we could directly target N_2 fluxes using a Monte Carlo approach. The statistical formulation used here is constructed specifically for the mechanisms described by Duncan et al. (2013). Thus, the detailed threshold limits could change under other denitrification HSHMs cases, such as the case presented in~~ Alternatively, numerical modeling approaches can be used to construct the dynamic indicators based on the critical conditions at riparian hollows ($\boldsymbol{\Omega}^*$), where we could directly target N_2 fluxes using a Monte Carlo approach. The statistical formulation used here is constructed specifically for the mechanisms described by Duncan et al. (2013). Thus, the detailed threshold limits could change under other denitrification HSHMs cases, such as the case presented in Hill et al. (2000)~~, who focus on desert landscapes, or the one by Harms and Grimm (2008), where the monsoon season is influential for the nitrogen transport.~~, who focus on desert landscapes, or the one by Harms and Grimm (2008), where the monsoon season is influential for the nitrogen transport. Nonetheless, the general formulation of HSHMs using indicators is still applicable.

3.3 HSHMs occuring when multiple dynamic processes converge in space

HSHMs can also be triggered by the confluence of multiple dynamic processes that lead to the convergence of complementary reactants at $\boldsymbol{\Omega}^*$. ~~Accumulation of complementary~~Complementary reactants ~~is~~can be mobilized and transported via different hydrologic flowpaths. They can converge at hot spot locations and trigger hot moments during the mixing. Following the statistical framework developed in this study, ~~Eq~~Eqs. (7) to (9) are suitable for this condition. In order to illustrate how the dynamic indicators are constructed, we consider here the case reported by Gu et al. (2012), where high biogeochemical activity was observed at the interface of groundwater and surface water during the stream stage fluctuations, which resulted in significant in-stream denitrification and NO_3^- removal.

In their study, hot spots form around the near-stream~~-~~ riparian subsurface during river stage fluctuations, where active biogeochemical reaction (e.g., denitrification) requires both O_2 depletion and the simultaneous presence

of NO_3^- and the dissolved organic carbon (DOC). Specifically, the spatiotemporal distribution of denitrification hot spots coincides with an O_2 depletion zone along the DOC infiltration flowpaths. In order to determine the mixing of groundwater and surface water during stage fluctuations, Gu et al. (2012) defined bank storage volume $V(t)$ and maximum bank storage volume V_{max}. The flood hydrograph was subdivided into the rising limbs, recession limbs and return flow, the latter representing the slow restitution of part of the water that infiltrated during the previous stages. Considering the different dynamics of these components, they observed that the largest infiltration rate occurred prior to the maximum stage rise, while $V_{max} = 5m^3m^{-1}$ (critical condition) occurred in the recession limb of the flood event. Instead, maximum return flow occurred toward the end of the recession curve before stream hydrograph stabilizes. Maximum NO_3^- rate removal occurred when return flow phase was almost complete and then decreased until the depletion of NO_3^-. Through statistical analysis, they found that V_{max}, viewed as an integrated index for hydrological exchange, could explain 64% of the variation in the NO_3^- removal. Thus, V_{max} can be used as the critical state to determine whether or not the hyporheic dynamics is significant to enhance relevant biogeochemical processes. In order for the hot moments to be significant, the stream-riparian zone should also be microbially active. Based on these conditions, the dynamic indicators can be constructed as follows:

$$P[I_d(\boldsymbol{\Omega}^*, t^*) = 1] = P\big[\, I_{d,Hydro}(\boldsymbol{\Omega}^*, t^*) = 1, I_{d,Chem}(\boldsymbol{\Omega}^*, t^*) = 1\big], \tag{14}$$

where $I_{d,Hydro}(\boldsymbol{\Omega}^*, t^*)$ represents the dynamic process induced by the hydrologic conditions (e.g., stage fluctuation), and $I_{d,Chem}(\boldsymbol{\Omega}^*, t^*)$ represents the dynamic process controlled by the transport and accumulation of chemical reactants. Based on the critical values or ranges, we formulate the indicators as follows:

$$\begin{aligned} I_{d,Hydro}(\boldsymbol{\Omega}^*, t^*) &= \begin{cases} 1, & Z_{V_{max}}(\boldsymbol{\Omega}^*, t^*) \geq 5m^3m^{-1} \\ 0, & otherwise \end{cases}, \\ I_{d,Chem}(\boldsymbol{\Omega}^*, t^*) &= \begin{cases} 1, & if\ C_{O_2}(\boldsymbol{\Omega}^*, t^*)\ is\ small\ and\ C_{NO_3^-}(\boldsymbol{\Omega}^*, t^*) > 0\ and\ C_{DOC}(\boldsymbol{\Omega}^*, t^*) > 0 \\ 0, & otherwise \end{cases}. \end{aligned} \tag{15}$$

Typically, because of the complexity of the processes, no analytical solutions are available for formulating the indicators. However, Monte Carlo simulations can be useful in constructing such indicators. For this case, an HSHM at any given location and time $(\boldsymbol{\Omega}^*, t^*)$ will only be triggered when all of the conditions are met and the ensemble mean of the indicator assumes the following form:

$$< I_d(\boldsymbol{\Omega}^*, t^*) > = \frac{1}{N}\sum_{i=1}^{N} I_{d,i}(\boldsymbol{\Omega}^*, t^*)\ , \tag{16}$$

where $I_{d,i}(\boldsymbol{\Omega}^*, t^*)$ is the value that the indicator assumes in the i^{th} realization and N is the total number of ~~simulations~~realizations.

Overall, our choices of the three studies should not limit the generalizability of the indicator statistics approach for deriving statistical formulations for HSHM applications. The critical conditions chosen to construct the indicators are determined solely on the findings from these selected studies, and they will vary under different scenarios.

4 HSHM applications in groundwater hydrology

~~Processes occurring within~~This section focuses on HSHMs in the subsurface ~~are important factors leading to~~for demonstration of linking HSHM ~~occurrences. Among others, these~~models with the contributing physical processes ~~include~~, such as the migration of groundwater carrying reducing substrates, nuclear waste transport within the subsurface, the accumulation and transport of dense non-aqueous phase liquid (DNAPL) and other biogeochemical processes. Some current modeling approaches that focus on subsurface HSHMs assume simplified hydrologic structures (e.g., homogeneous and isotropic domains) in quantifying ~~contaminant~~the fate and transport of solutes in the subsurface. However, such ~~an assumption neglects~~assumptions neglect the effect of the heterogeneity in the subsurface, ~~leading to the underestimation of~~potentially missing localized HSHMs arising as the combined effect of heterogeneity in physical and geochemical properties, and do not allow to assess uncertainties in the HSHM occurrences. ~~Thus, in this~~

This section~~, we focus~~ therefore focuses on ~~HSHM applications in groundwater hydrology~~HSHMs taking place in the subsurface, with a particular emphasis on the role of spatial variability ~~in the subsurface. Specifically, we consider several situations often encountered in groundwater contamination studies and present the indicator statistical formulations of HSHMs. With these results, we can determine~~of the ~~probability of HSHMs occurrences in~~hydrologic parameters. Section 4.1 illustrates the potential of subsurface ~~at a given time and space. Further, we are able to determine how~~heterogeneity for triggering and timing of HSHMs. In section 4.2, we develop closed-form analytical solutions for HSHM probability. In doing this, we demonstrate the linking between our indicator model and the physics of the HSHMs in the subsurface. In section 4.3 we demonstrate applications under various conditions of spatial variability ~~influences HSHM occurrences and how this is translated into environmental health risks~~.

4.1 Importance of spatial variability in the subsurface

The heterogeneous structure of hydraulic conductivity leads to significant variability in the ~~contaminant transport in the subsurface, which further results in the heterogeneity of biogeochemical cycling, such as the development of NRZs, reactive facies, and heterogeneity in aquifers' reactivity (Li et al., 2010; Loschko et al., 2016; Sassen et al., 2012; Wainwright et al., 2015).~~

transport of solutes in the subsurface, which couples with heterogeneous geochemical properties leading to a spatially variaying reactivity (Arora et al., 2019b; Loschko et al., 2016; Sassen et al., 2012; Wainwright et al., 2015). Figure 2 demonstrates the uncertainty associated with HSHMs by looking at the flow fields in two-dimensional log-hydraulic conductivity ($Y = ln(K)$) fields with streamlines resulting from a uniform mean head gradient, left to right. The three panels differ in terms of the variance, σ_Y^2, of the log-conductivity. The covariance function used for generating the fields is exponential and isotropic. σ_Y^2 is shown to have a profound impact upon the conductivity field. As the variance increases, regions of high and low log-conductivity emerge, creating preferential flow paths bypassing the low conductivity zones as shown by particle trajectories. At smaller variance (i.e., $\sigma_Y^2 = 0.1$), particles mainly travel along the mean flow direction with very limited departure from the mean trajectory, which are the straight lines connecting the left and right boundaries. In this situation, the arrival times of solute particles to a critical ~~locations~~location (i.e., $\boldsymbol{\Omega}^*$~~))~~, where for example geochemical conditions are favorable to certain types of reactions to occur) are predictable. With large variances (i.e., $\sigma_Y^2 = 2$), the streamlines assume a very irregular, hard-to-predict

geometry, and we can observe the emergence of flow channels, where particles can move fast, next to stagnant flow regions. Arrival times become more uncertain, because the exact geometry of the streamlines is hard to predict unless the Y field is known deterministically. However, since this is never the case, in another equally likely realization of the Y field, the situation may be totally different, resulting in significant uncertainties in predicting the particle travel times. Thus, spatial variability of log-conductivity is a major uncertainty-inducing factor, and by extension, obviating the need for stochastic modeling of HSHMs in situations where the associated processes and attributes are subject to uncertainty. In the following sections, we will present illustrative examples to analyze how subsurface spatial variability influences $< I_{HSHM}(\boldsymbol{\Omega}^*, t^*) >$, including variance and anisotropy ratio of the log-conductivity.

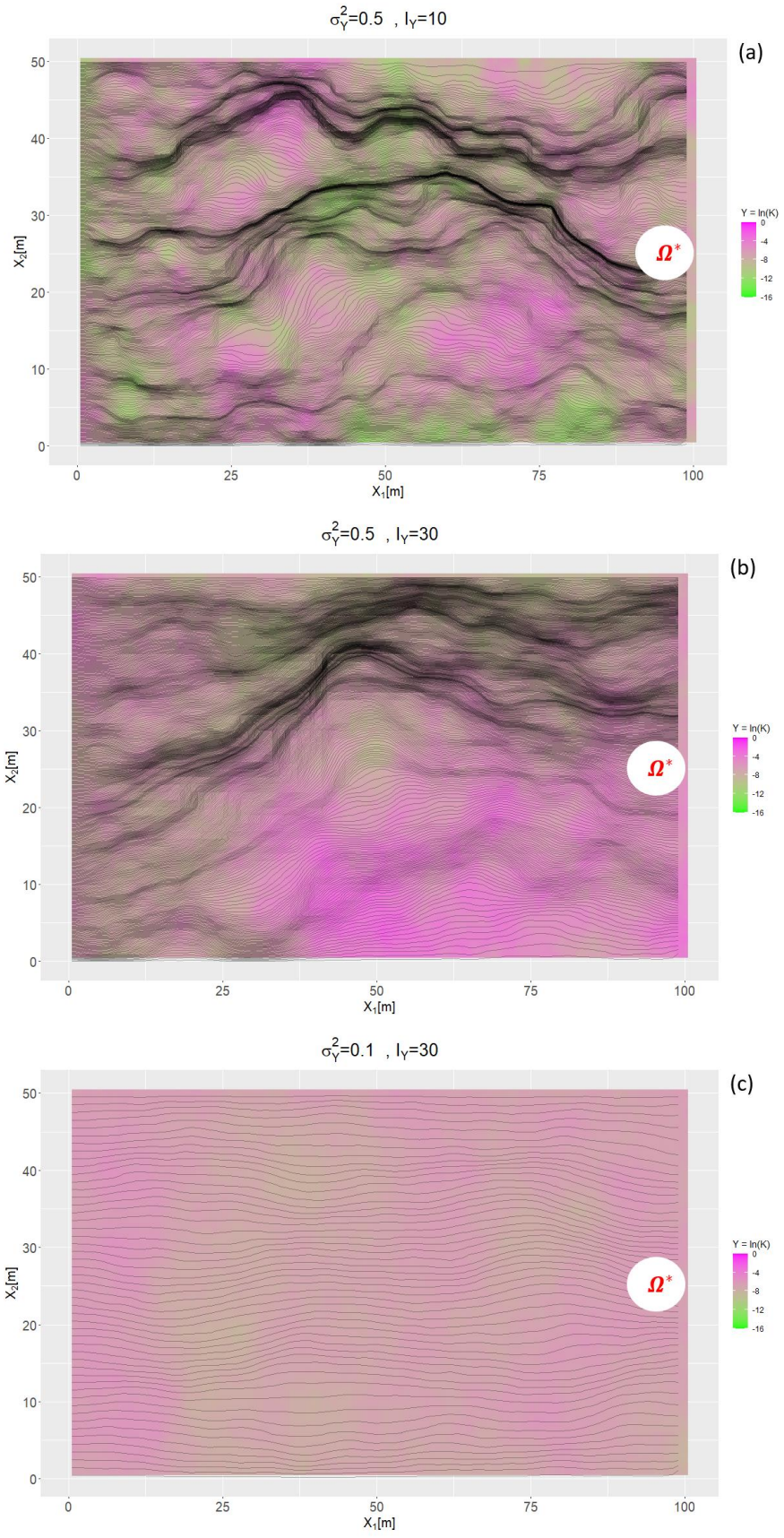
σ_Y^2=0.5 , I_Y=10
(a)
Ω^*
Y = ln(K)
0
-4
-8
-12
-16
X_2[m]
X_1[m]
0
25
50
75
100
σ_Y^2=0.5 , I_Y=30
(b)
Ω^*
σ_Y^2=0.1 , I_Y=30
(c)
Ω^*

Figure 2. Illustrative example of a heterogeneous log-hydraulic conductivity field and solute particle transport. Black lines represent simulated particle travel paths. A left to right hydraulic gradient of 0.1 is applied. Mean of log-conductivity is set at -3. Note color scales for log-conductivity are consistent in all three panels.

4.2 ~~Case studies~~ Illustrative example and ~~expansions of indicators~~indicator formulation

In this section we illustrate the proposed indicator approach by means of synthetic case studies developed by using methods of stochastic hydrogeology. The choice of the synthetic case studies does not limit our approaches to broader applications where stochastic modeling with Monte Carlo simulations are applicable. ~~**4.2.1 Single particle I_a within Ω^***~~

Figure 3 displays the configuration of this case example. Consider the case of ~~a~~an instantaneous point source release of ~~non-reactive tracer originated from $(\boldsymbol{x_0}, t_0)$. The dynamic indicator depends on a particle being within $\boldsymbol{\Omega^*}$~~ a target compound at the location $\boldsymbol{x_0}$ and time t_0. HSHMs are triggered at any $(\boldsymbol{\Omega^*}, t^*$ ~~or not. If local (pore scale) dispersion~~) if the solute is present. Consider the hot spot $(\boldsymbol{\Omega^*})$ to be confined within the following volume: $w_1 \le x_1 \le w_1'; w_2 \le x_2 \le w_2'; w_3 \le x_3 \le w_3'$ ~~neglected,~~, the dynamic indicator is therefore defined as follows:

$$I_d(\boldsymbol{\Omega^*}, t^*) = \begin{cases} 1, & if\ \boldsymbol{X}(t^*) \subseteq \boldsymbol{\Omega^*}\ at\ t^* \\ 0, & otherwise \end{cases}. \quad (17)$$

~~Given that the particle does not change its volume while traveling.~~The injected solute can be modelled in a Lagrangian way as a particle moving according to the velocity field without changing its volume. The latter is the consequence of neglecting pore scale dispersion. The expected value of this dynamic indicator at t^* is therefore:

$$< I_d(\boldsymbol{\Omega^*}, t^*) >= \int_{\Omega^*} f_{\boldsymbol{X}(t^*)}(\boldsymbol{a}|\boldsymbol{x}_0, t_0) d\boldsymbol{a}, \quad (18)$$

where $f_{\boldsymbol{X}(t^*)}(\boldsymbol{a}|\boldsymbol{x}_0, t_0)$ is the probability distribution function (pdf) of the particle's trajectory at ~~t^* (Dagan and Nguyen, 1989; Rubin, 2003). Other situations may be addressed by using the same framework. For example, for an instantaneous injection within a source volume V_0, the ensemble mean of the dynamic indicator assumes the following form:~~

~~$$< I_a(\boldsymbol{\Omega^*}, t^*) >= \frac{1}{V_0} \int_{V_0} \int_{\Omega^*} f_{\boldsymbol{X}(t^*)}(\boldsymbol{a}|\boldsymbol{x}_0, t_0) d\boldsymbol{a} d\boldsymbol{x}_0. \quad (19)$$~~

~~**4.2.2 Concentration-based I_a within Ω^***~~

~~When considering local dispersion, or in case of a reactive tracer, the condition that the particle is inside the volume $\boldsymbol{\Omega^*}$ does not suffice to define the dynamic indicator and a concentration threshold C_{th} should be introduced:~~

~~$$I_d(\boldsymbol{\Omega^*}, t^*) = \begin{cases} 1, & if\ \boldsymbol{X}(t^*; \boldsymbol{x}_0, t_0) \subseteq \boldsymbol{\Omega^*}\ and\ C(\boldsymbol{X}, t^*) > C_{th} \\ 0, & otherwise \end{cases}. \quad (20)$$~~

~~In the absence of local dispersion and for a reactive solute decaying at a (spatially) constant rate k, the ensemble mean assumes the following expression (Cvetkovic and Shapiro, 1990):~~

~~$$< I_a(\boldsymbol{\Omega^*}, t^*) >= \left\{1 - H\left[t^* - \frac{1}{k}\ln\left(\frac{C_0}{C_{th}}\right)\right]\right\} \int_{\Omega^*} f_{\boldsymbol{X}(t^*)}(\boldsymbol{a}|\boldsymbol{x}_0, t_0) d\boldsymbol{a}, \quad (21)$$~~

~~where C_0 is the initial concentration and $H[\cdot]$ is the Heaviside step function. The ensemble mean (21) is the product of the probability that the particle assumes a concentration larger than the threshold at t^* (given that reaction rate k is constant, this probability is either 0 or 1) and the probability that at the same time t^* the particle is within the hot spot~~

$\boldsymbol{\Omega}^*$. In other words, Eq. (21) expresses the fact that a particle inside $\boldsymbol{\Omega}^*$ contributes to the hot moment only if its concentration is greater than the threshold. Equation (21) can be generalized to the cases of instantaneous injection into a source of volume V_0, as discussed before for the non-reactive case. For other complex situations, such as that in which k is spatially variable and complex reaction networks, the ensemble mean of the indicators can be addressed by Eq. (16) in a Monte Carlo framework.

4.2.3 Assessing the duration of hot moment and probabilities

The probability that the hot moment persists over the interval $[t_1, t_2]$ at $\boldsymbol{\Omega}^*$ can be formally computed as follows:

$$< I_d(\boldsymbol{\Omega}^*, t_1, t_2) >= P(t_1, \boldsymbol{\Omega}^*) P(t_2 | t_1, \boldsymbol{\Omega}^*), \quad (22)$$

where $P(t_1, \boldsymbol{\Omega}^*)$ is the probability that the particle is inside $\boldsymbol{\Omega}^*$ at time $t^* = t_1$ and $P(t_2 | t_1, \boldsymbol{\Omega}^*)$ is the probability that the particle is still inside $\boldsymbol{\Omega}^*$ at time $t^* = t_2$, provided that at time t_1, it was also inside $\boldsymbol{\Omega}^*$. If the particle exits $\boldsymbol{\Omega}^*$ during interval $[t_1, t_2]$, this time interval will not be qualified as hot moment; and thus the probability computation needs to ensure the particle stays within $\boldsymbol{\Omega}^*$ during the entire time interval.

Under the First-Order Approximation (FOA) (see e.g., Dagan, 1989; Gelhar 1993; Rubin, 2003), the pdf of the particle displacement is normal with mean $< \boldsymbol{X}(t^*; \boldsymbol{x}_0, t_0) >$ and auto-covariance tensor of the residual displacements $\boldsymbol{X}'(t^*) = \boldsymbol{X}(t^*) - \langle \boldsymbol{X}(t^*) \rangle$ defined by $\boldsymbol{X}_{ij}(t^*; \boldsymbol{x}_0, t_0) = \langle \boldsymbol{X}'_i(t^*; \boldsymbol{x}_0, t_0) \boldsymbol{X}'_j(t^*; \boldsymbol{x}_0, t_0) \rangle$, $i, j = 1, 2, 3$. For simplicity in the following, we assume $\boldsymbol{x}_0 = 0$ *and* $t_0 = 0$. Under these assumptions,

$$< I_d(\boldsymbol{\Omega}^*, t_1, t_2) >= \int_{\boldsymbol{\Omega}^*} \int_{\boldsymbol{\Omega}^*} f_{\boldsymbol{X}(t_1)}(\boldsymbol{a}) f^c_{\boldsymbol{X}(t_2)}(\boldsymbol{b} | \boldsymbol{X}(t_1) = \boldsymbol{a})\, d\boldsymbol{b}\, d\boldsymbol{a}, \quad (23)$$

where the conditional pdf $f^c_{\boldsymbol{X}(t_2)}(\boldsymbol{b} | \boldsymbol{X}(t_1) = \boldsymbol{a})$ is multi normally distributed with conditional mean and variance tensor given by

$$\langle \boldsymbol{X}(t_2) | \boldsymbol{X}(t_1) = \boldsymbol{a}) \rangle = < \boldsymbol{X}(t_2) > + Cov[\boldsymbol{X}'(t_2), \boldsymbol{X}'(t_1)] \cdot Var[\boldsymbol{X}'(t_1)]^{-1} \cdot (\boldsymbol{a} - < \boldsymbol{X}(t_1) >), \quad (24)$$

and

$$\boldsymbol{\sigma}(t_1, t_2) = Var[\boldsymbol{X}'(t_2)] - Cov[\boldsymbol{X}'(t_2), \boldsymbol{X}'(t_1)] \cdot Var[\boldsymbol{X}'(t_1)]^{-1} \cdot Cov[\boldsymbol{X}'(t_1), \boldsymbol{X}'(t_2)], \quad (25)$$

respectively, which further yields the following,

$$f^c_{\boldsymbol{X}(t_2)}(\boldsymbol{b} | \boldsymbol{X}(t_1) = \boldsymbol{a}) = \exp\left[-\frac{1}{2} [\boldsymbol{b} - \langle \boldsymbol{X}(t_2) | \boldsymbol{X}(t_1) = \boldsymbol{a}) \rangle]^T \cdot \boldsymbol{\sigma}(t_1, t_2)^{-1} \cdot [\boldsymbol{b} - \langle \boldsymbol{X}(t_2) | \boldsymbol{X}(t_1) = \boldsymbol{a}) \rangle] \right] \cdot \{8\, \pi^3 \cdot |\boldsymbol{\sigma}(t_1, t_2)|\}^{-\frac{1}{2}}, \quad (26)$$

where $|\,|$ indicates the determinant, *exp* is the exponential function and the exponent T indicates the transpose of the vector.

In Eq. (24) and (25), $\boldsymbol{X}'(t^*) = \boldsymbol{X}(t^*) - \langle \boldsymbol{X}(t^*) \rangle$ stands for the departure of the particle's displacement with respect to the ensemble mean trajectory, and $Var[\boldsymbol{X}]^{-1}$ is the auto-covariance tensor of the residual displacement whose elements are defined above. Similarly, $Cov[\boldsymbol{X}'(t_1), \boldsymbol{X}'(t_2)]$ is the covariance tensor of residual displacement

which elements are: $\boldsymbol{X}_{ij}(t_1, t_2; \boldsymbol{x}_0, t_0) = \langle X_i^x(t_1)\, X_j^x(t_2)\rangle, i, j = 1, 2, 3$. Note that in the general three-dimensional case $\langle \boldsymbol{X}(t_2)|\, \boldsymbol{X}(t_1) = \boldsymbol{a}\rangle$ is a three-dimensional vector and $\boldsymbol{\sigma}(t_1, t_2)$ is a 3×3 second-order tensor.

For $t_2 \to t_1$, $f_{X(t_2)}[\boldsymbol{b}|\boldsymbol{X}(t_1) = \boldsymbol{a}] \to \delta(\boldsymbol{b})$, where $\delta(\cdot)$ is the Dirac Delta, such that $P(t_2|t_1, \boldsymbol{\Omega}^*) \to 1$. On the other hand, for $t_2 \gg t_1$, $Cov[\boldsymbol{X}^x(t_1), \boldsymbol{X}^x(t_2)] \to 0$ and $P(t_2|t_1, \boldsymbol{\Omega}^*) \to P(t_2, \boldsymbol{\Omega}^*)$ the marginal probability that the particle is within $\boldsymbol{\Omega}^*$ at time $t^* = t_2$. Equations (23) to (26) are obtained under the FOA approximation and assuming that the particle can enter $\boldsymbol{\Omega}^*$ only once. Such assumption is needed to obtain analytical solutions and is reasonable for situations with small to mild subsurface heterogeneity (e.g., $\sigma_Y^2 \leq 1.6$), such as the cases presented in Bellin et al. (1992, 1994); Cvetkovic et al. (1992). In particular, FOA assumes small heterogeneity and under this assumption the particle trajectory deviates slightly from its ensemble mean, which is directed along the regional hydraulic head gradient. For a regular volume $\boldsymbol{\Omega}^*$, this reduces the probability of the particle entering more than once the hot spot. This probability reduces further if in horizontal and vertical transverse directions $\boldsymbol{\Omega}^*$ is much larger than the respective integral scales, because the probability of observing negative longitudinal velocity components (i.e., along the mean flow field) is much smaller than in the transverse directions (Bellin et al., 1992) and vanishes as formation heterogeneity reduces.

If the hotspot $\boldsymbol{\Omega}^*$ is the volume confined between two planes at $x_1 - \frac{l_1}{2}$ and $x_1 + \frac{l_1}{2}$, with the other two dimensions much larger than the transverse horizontal and vertical integral scales: $l_2 \gg I_2$, $l_3 \gg I_3$, Eq. (24) simplifies to:

$$< I_d(\boldsymbol{\Omega}^*, t_1, t_2) >= \int_{x_1-\frac{l_1}{2}}^{x_1+\frac{l_1}{2}} \int_{x_1-\frac{l_1}{2}}^{x_1+\frac{l_1}{2}} f_{X_1(t^*)}(a_1) f^c_{X_1(t^*)}(\, b_1|X_1(t_1) = a_1)\, db_1\, da_1, \qquad (27)$$

where X_1 is the longitudinal component of the particle's trajectory and $f^c_{X_1(t^*)}$ is its conditional pdf, which is normal with conditional mean and variance given by

$$\mu[a_1] = \langle X_1(t_2)|\, X_1(t_1) = a_1)\rangle = < X_1(t_2) > + \frac{X_{11}(t_1, t_2)}{X_{11}(t_1)} (X_1(t_1) - < X_1(t_1) >), \qquad (28)$$

and

$$\sigma^2(t_1, t_2) = X_{11}(t_2) - \frac{X_{11}(t_1, t_2)^2}{X_{11}(t_1)}, \qquad (29)$$

respectively. Consequently, $f_{X^c(t^*)}$ in Eq. (27) assumes the following form:

$$f^c_{X_1(t^*)}(b_1|X_1(t_1) = a_1) = \frac{1}{\sqrt{2\,\pi\,\sigma(t_1, t_2)}} \exp\left[-\frac{1}{2}(b_1 - \mu[a_1])^2\, \sigma(t_1, t_2)^{-1}\right]. \qquad (30)$$

Substituting Eq. (30) into Eq. (27) allows us to compute $< I_d(\boldsymbol{\Omega}^*, t_1, t_2) >$. For situations where the FOA assumptions are not valid (e.g., large heterogeneity), Monte Carlo simulation framework is still applicable as alternative approach to construct the dynamics indicators (see Eq. 16).

4.3 Illustrative example and indicator formulation

Following sections 4.1 and 4.2, we present here synthetic case studies that demonstrate the statistical formulation of the indicators using methods developed in stochastic hydrogeology. The choice of the synthetic case studies does not limit our approaches to broader applications where stochastic modeling with Monte Carlo simulations are applicable.

~~In most applications, the locations of hot spots ($\boldsymbol{\Omega}^*$) are determined by static indicators, such as riparian hollows (Duncan et al., 2013), reactive facies (Sassen et al., 2012), and NRZs (Wainwright et al., 2015). The static indicator is constructed according to the corresponding critical conditions provided by ancillary data such as topography, remote sensing, and/or geophysical data. Hence, in this case, assuming the boundaries of $\boldsymbol{\Omega}^*$ are determined by a static indicator, we consider a hot spot ($\boldsymbol{\Omega}^*$) to be confined within the following volume: $w_1^t \leq x_1 \leq w_1^t; w_2^t \leq x_2 \leq w_2^t; w_3^t \leq x_3 \leq w_3^t$~~time t^* (Dagan and Nguyen, 1989; Rubin, 2003). If we also assume steady, uniform in the average flow with mild heterogeneity of the log hydraulic conductivity field with Gaussian displacement pdf—then we can compute $< I_{HSHM}(\boldsymbol{\Omega}^*, t^*) >$ analytically using the following equation:

~~.~~

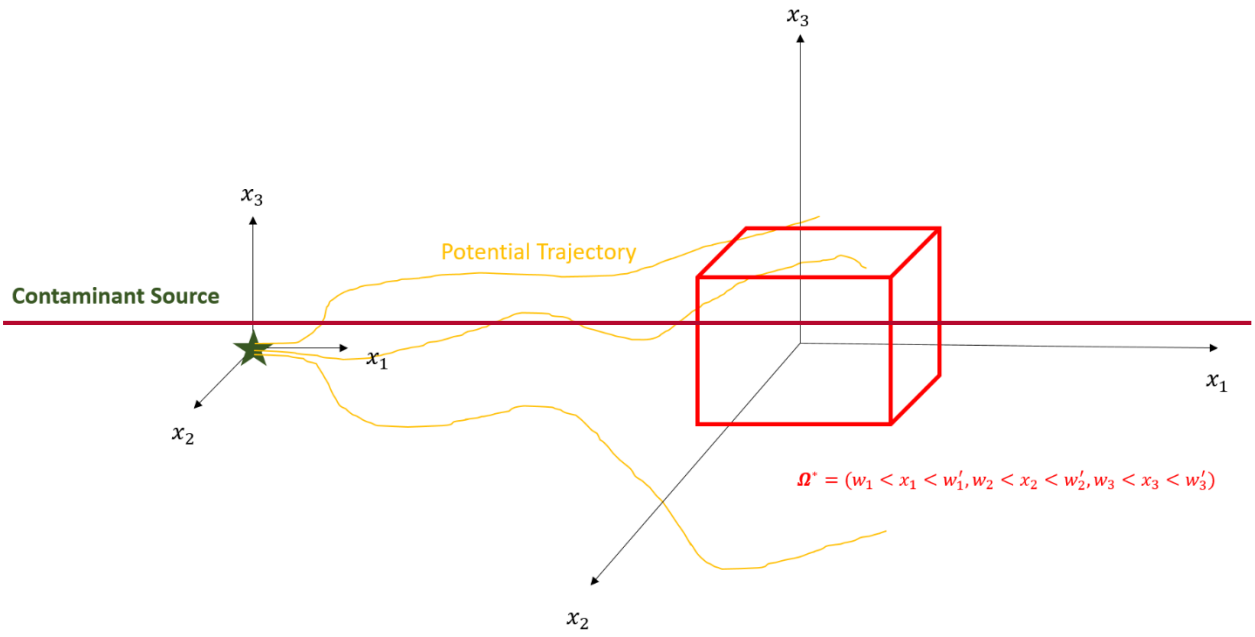

~~Figure 3. Configuration of the synthetic case study~~

~~Given this case, the hot moment will be triggered only when the contaminant particle is found within $\boldsymbol{\Omega}^*$. The probability of finding the contaminant particle within $\boldsymbol{\Omega}^*$ is given by~~

$$~~prob\{\boldsymbol{X}(t^*) \subseteq \boldsymbol{\Omega}^*\}~~$$

$$~~= \prod_{i=1}^{m} prob\{w_i \leq X_i(t^*) \leq w_i^t\} = \prod_{i=1}^{m} \int_{w_i}^{w_i^t} f_{X_i(t^*)}(a_i|x_0, t_0)da_i,~~ \quad ~~(33)$$

~~where m denotes the space dimensionality. Equation (33) defines the dynamic indicator for this case. If $\boldsymbol{\Omega}^*$ is already identified as a hot spot location, then$P(I_{HSHM}(\boldsymbol{\Omega}^*, t^*) = 1) =< I_{HSHM}$ Eq. (33) provides $< I_{HSHM}(\boldsymbol{\Omega}^*, t^*) >$. Otherwise, the static indicator should be incorporated to determine the boundaries of $\boldsymbol{\Omega}^*$ in order to compute $< I_{HSHM}(\boldsymbol{\Omega}^*, t^*) >$ as shown in Eq. (10) where geophysical data is used to identify the spatial context of $\boldsymbol{\Omega}^*$. If we also assume steady, uniform in the average flow with mild heterogeneity of the log hydraulic conductivity field with Gaussian displacement pdf—then we can compute $< I_{HSHM}(\boldsymbol{\Omega}^*, t^*) >$ analytically using the following equation:~~

$$~~< I_{HSHM}(\boldsymbol{\Omega}^*, t^*) >=< I_s(\boldsymbol{\Omega}^*) > < (I_d(\boldsymbol{\Omega}^*, t^*) >~~$$

$$= prob(I_d(\boldsymbol{\Omega}^*, t^*) = 1) = prob\{X(t^*) \subseteq \boldsymbol{\Omega}^*\}$$

$$= \prod_{i=1}^{m} \int_{w_i}^{w_i'} f_{X_i(t^*)}(a_i|x_0, t_0)da_i = \int_{w_1}^{w_1'} f_{X_1(t^*)}(a_1|x_0, t_0)da_1 \int_{w_2}^{w_2'} f_{X_2(t^*)}(a_2|x_0, t_0)da_2 \int_{w_3}^{w_3'} f_{X_3(t^*)}(a_3|x_0, t_0)da_3$$

$$= \frac{1}{(2\pi)^{\frac{3}{2}}\sqrt{X_{11}(t^*)X_{22}(t^*)X_{33}(t^*)}} \int_{w_1}^{w_1'} \exp\left[-\frac{1}{2}\frac{(a_1 - Ut^*)^2}{X_{11}(t^*)}\right]da_1$$

$$\cdot \int_{w_2}^{w_2'} \exp\left[-\frac{1}{2}\frac{a_2^2}{X_{22}(t^*)}\right]da_2 \int_{w_3}^{w_3'} \exp\left[-\frac{1}{2}\frac{a_3^2}{X_{33}(t^*)}\right]da_3. \quad (3419)$$

which can be integrated to yield :

$$\cancel{< I_{HSHM}} P(I_{HSHM}(\boldsymbol{\Omega}^*, t^*) = 1) =< I_{HSHM}(\boldsymbol{\Omega}^*, t^*) >= \frac{1}{8}\left[\text{erfc}\left(\frac{w_1 - Ut^*}{\sqrt{2X_{11}(t^*)}}\right) - \text{erfc}\left(\frac{w_1' - Ut^*}{\sqrt{2X_{11}(t^*)}}\right)\right]$$

$$\cdot \left[\text{erfc}\left(\frac{w_2}{\sqrt{2X_{22}(t^*)}}\right) - \text{erfc}\left(\frac{w_2'}{\sqrt{2X_{22}(t^*)}}\right)\right]\left[\text{erfc}\left(\frac{w_3}{\sqrt{2X_{33}(t^*)}}\right) - \text{erfc}\left(\frac{w_3'}{\sqrt{2X_{33}(t^*)}}\right)\right]. \quad (3520)$$

~~The form of the displacement variances is controlled by the spatial distribution of the hydraulic conductivity in the subsurface. Equations (A4)-(A6) of the appendix show the displacement variances for an axisymmetric exponential covariance function of the log-conductivity (A3).~~

~~4.4 Implications for HSHMs~~

For simplifiy, but without lack of generality, in Eq. (20) we assumed $\boldsymbol{x}_0 = (0,0,0)$. The displacement variances $X_{ii}, i = 1,2,3$ depends on the spatial distribution of the hydraulic conductivity in the subsurface. Eqs. (A4) to (A6) present the displacement variances for an axisymmetric exponential covariance function of the log-conductivity (A3) are given in the Appendix A. In Eqs. from (A7) to (A19), we have provided derivations of indicator formulations for other HSHMs scenarios, including indicator formulation for complex concentration thresholds and indicator formulation for hot moment durations. Notice that in obtaining Eq. (20) we postulated ergodicity, which in practical terms reflects the actual situation of an instantaneous injection into a source zone with transverse dimension much larger than the integral scale of the hydraulic conductivity (Dagan, 1990), such that the ensemble mean is representative of the effects of the actual, but unknown, distribution of hydraulic conductivity.

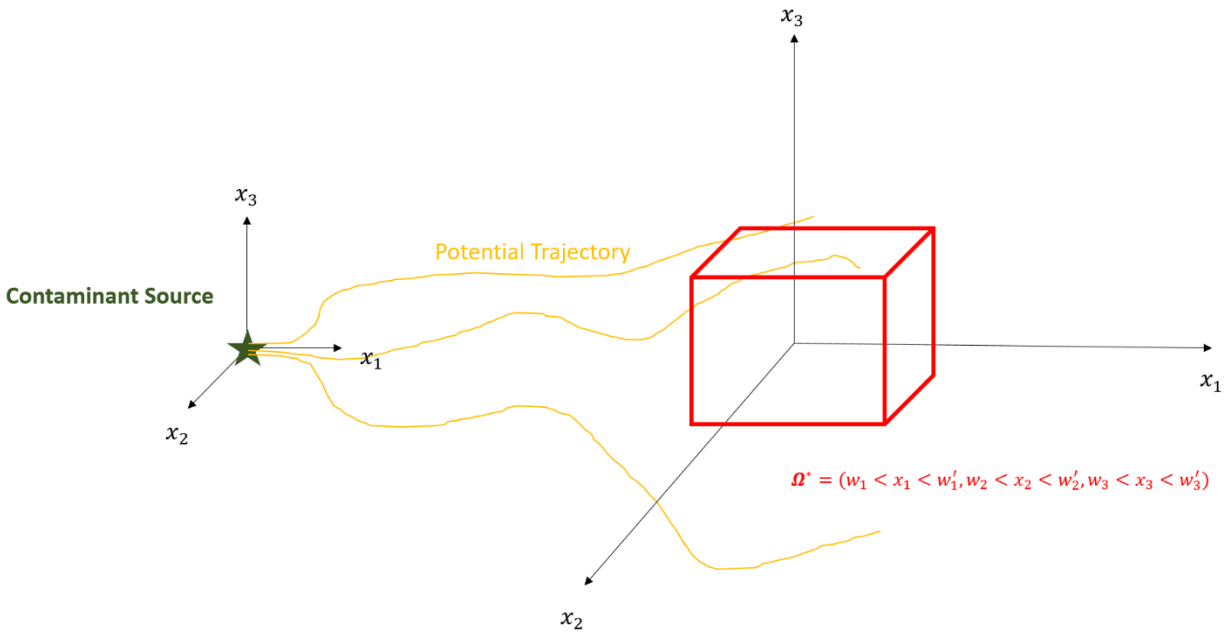

Figure 3. Configuration of the synthetic case study. x_1, x_2 and x_3 represent the longitudinal, transverse and vertical directions, respectively. $w_1, w_1', w_2, w_2', w_3$ and w_3' are the coordinates that set up the volume of $\boldsymbol{\Omega}^*$

4.3 Probability of HSHM occurrence controlled by subsurface heterogeneity

In the following sections, we present the results from the case study described in section 4.3. Specifically, in section 4.43.1 and 4.43.2, we explore how heterogeneity of log-hydraulic conductivity influences the probability of HSHM occurrences. To make results as general as possible, lengths are made dimensionless with respect to the integral scales (I_{Yh} in the two horizontal directions and I_{Yv} in the vertical one) and time with respect to the following advective time scale: I_{Yh}/U, where U is the mean velocity). In the following, we explore the effect of the remaining parameters, i.e. the anisotropy ratio $e = \frac{I_{YV}}{I_{YH}}$ and the variance of the log-conductivity σ_Y^2, on the emergence of HSHM. We placed $\boldsymbol{\Omega}^*$ along the mean trajectory at $(21I_{YH}, 0, 0)$ with dimensions as $(2I_{YH}, 2I_{YH}, 2I_{YV})$. The dimensions of the hot spot are therefore of two integral scales in the three coordinate directions (x_1, x_2, x_3) and is placed at a dimensionless distance of 21 from the point source.

4.43.1 Dependece of $< I_{HSHM}(\Omega^*, \tau) > P(I_{HSHM}(\Omega^*, \tau) = 1)$ on variance in the spatial correlation structure of the log-conductivity

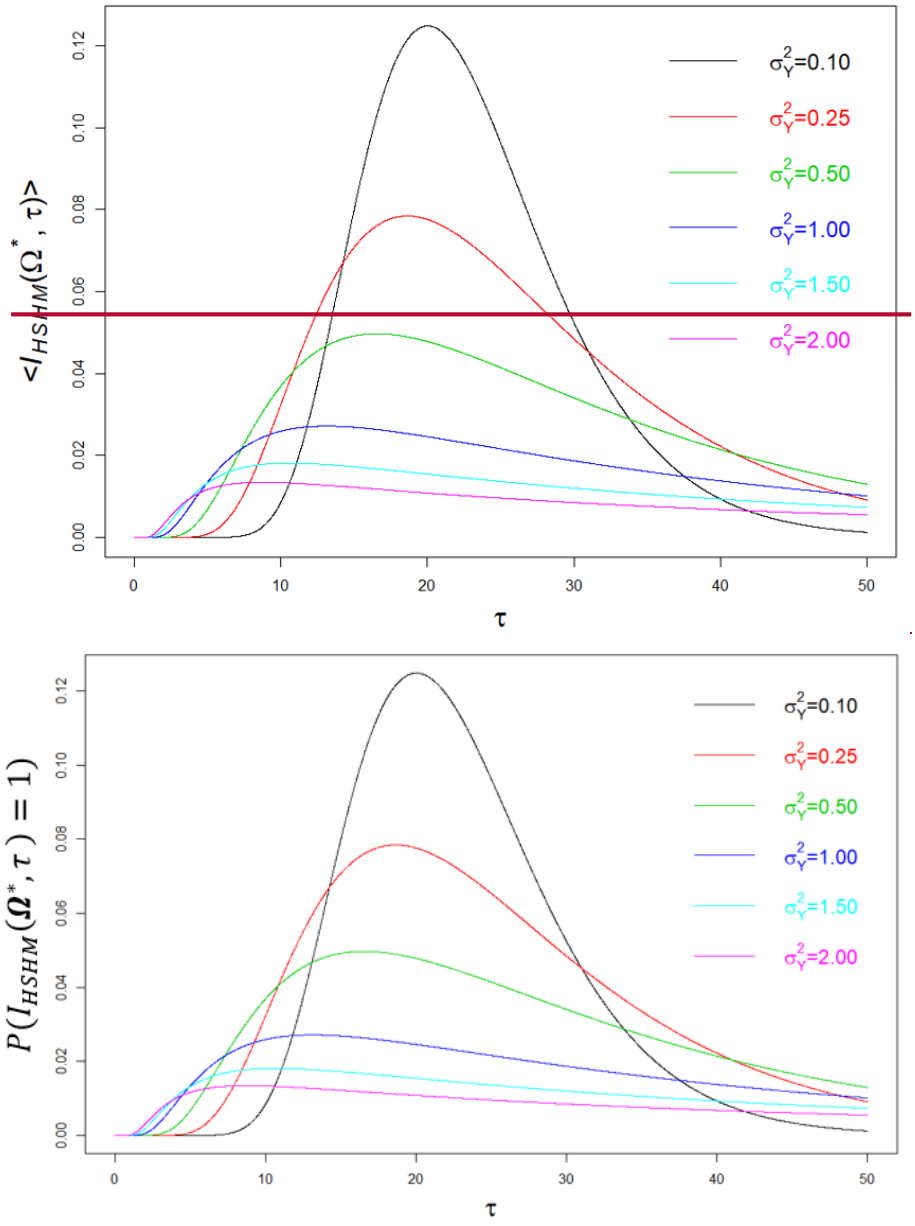

Figure 4. Dependence of $< I_{HSHM}(\Omega^*, \tau) > P(I_{HSHM}(\Omega^*, \tau) = 1)$ on σ_Y^2 Isotropic heterogeneity ($\sigma = 1$time (τ) and on the particle moments given by Eqs. (A7) and (A8)) was considered to investigatelevel of spatial variability of the dependence of $< I_{HSHM}(\Omega^*, \tau) >$ on log-hydraulic conductivity (σ_Y^2)

Figure 4 shows $P(I_{HSHM}(\Omega^*, \tau) = 1)$, which is the propability that a HSHM is triggered at Ω^* and the dimensionless time $\tau = \frac{tU}{I_{Yh}}$, for a few values of σ_Y^2. Here, $I_{HSHM}(\Omega^*, \tau)$ with results presented $= 1$ represents the situation in Figure 4. $\tau = tU/I_{Yh}$ is the dimensionless time.which a HSHM is triggered. At early time (e.g., $\tau < 5$), larger probability $< I_{HSHM} P(I_{HSHM}(\Omega^*, \tau) > = 1)$ is observed with increase in σ_Y^2. At intermediate time, i.e., at times comparable with the mean travel time $\tau = 21$, $< I_{HSHM} P(I_{HSHM}(\Omega^*, \tau) > = 1)$ is inversely

proportional to σ_Y^2. At late time (e.g., $\tau > 40$), the largest ~~$< I_{HSHM} P(I_{HSHM}(\boldsymbol{\Omega}^*, \tau) >= 1)$~~ occurs at intermediate σ_Y^2. We observe that σ_Y^2 regulates the timing of the peak in ~~$< I_{HSHM} P(I_{HSHM}(\boldsymbol{\Omega}^*, \tau) >= 1)$~~, which is located in the proximity of the mean travel time, $\tau = 21$, for weak heterogeneity, and shifts towards earlier times as σ_Y^2 increases. From the practical perspective, Figure 4 shows the probability of developing a HSHM at the identified position $\boldsymbol{\Omega}^*$ at the given time τ.

These effects relate to the relationship between travel times (from the source to $\boldsymbol{\Omega}^*$) and σ_Y^2. The key point to note is that σ_Y^2 controls the spread of the travel time around ~~the~~its mean ~~travel time. Larger variance enhance~~value. A larger σ_Y^2 enhances channeling effects ~~(Fiori and Jankovic, 2012; Moreno and Tsang, 1994, also in Figue 2), which in turn enable earlier arrival times. But at the same time, large σ_Y^2 also leads to the low-conductivity zones. Streamlines of the solute tend to bypass low hydraulic conductivity zones, however, the small amount of solute that actually penetrates these zones by~~(Fiori and Jankovic, 2012; Moreno and Tsang, 1994, also in Figure 2), which in turn enable earlier arrival times. But at the same time, it also leads to the emergence low-conductivity zones with low velocity or stagnant groundwater. The solute tends to bypass low hydraulic conductivity zones, as shown by the streamlines depicted in Figure 2, however, the small amount of solute that actually penetrates these zones by slow advection and diffusion gets trapped for long time before being released and this results in an extended tailing with low concentration ~~and therefore low $< I_{HSHM}(\boldsymbol{\Omega}^*, \tau) >$.~~, which increases the probability of observing a HSHM at later times. Thus, with an increase in σ_Y^2, we notice an increase in the probability to observe both increasingly earlier and increasingly delayed arrival times, which widens the probability distribution. On the contrary at small variance, particles deviate little from the ensemble mean trajectory, because of the small contrast in conductivity between high and low conductivity zones. This results in small particle spreading and travel times that differ only slightly from the mean travel time ($\tau = 21$), and a probability distribution less spread around the mean, where the peak is observed.

In summary, hydraulic conductivity contrast between low and high conductive lithofacies increases with σ_Y^2 leading to the emergence of organized high conductivity pathways sneaking through surrounding low conductivity zones with the latter acting as "trapping" elements. This causes the emergence of both early and late arrival times, with the consequent larger probability of triggering HSHMs at early and later times, with respect to the case of low heterogeneity. Early arrival times are controlled by the connected high conductivity pathways and the late arrival times are influenced by the low conductivity zones, which act as low-release reservoirs for solutes.

4.~~4.1~~3.2 Dependece of ~~$< I_{HSHM} P(I_{HSHM}(\Omega^*, \tau) >= 1)$~~ on on anisotropy in the spatial correlation structure of the log-hydraulic conductivity

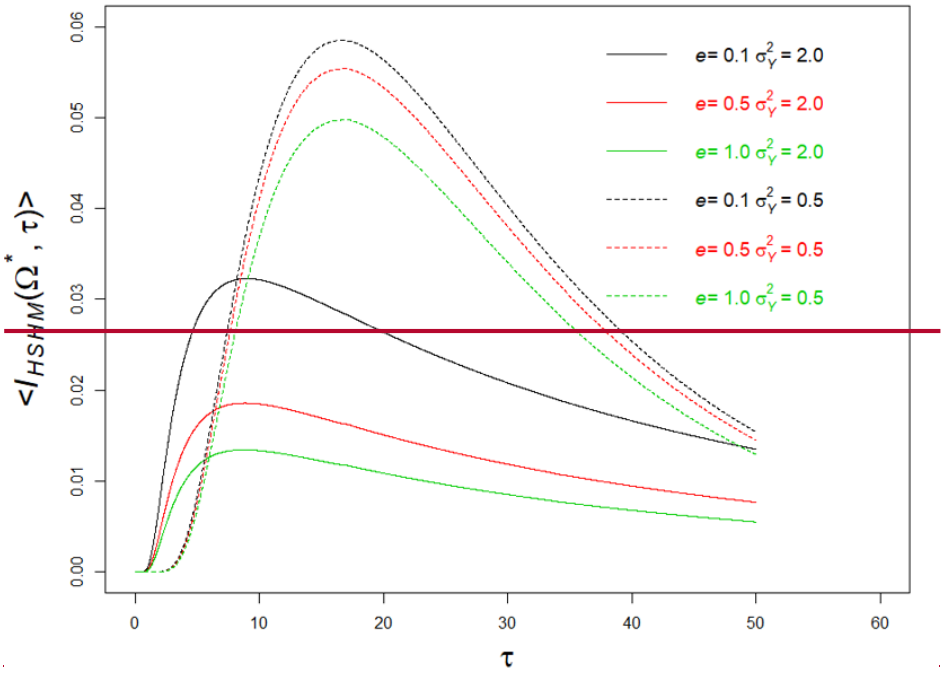

~~Figure 5. Dependence of $< I_{HSHM}(\Omega^*, \tau) >$ on e~~

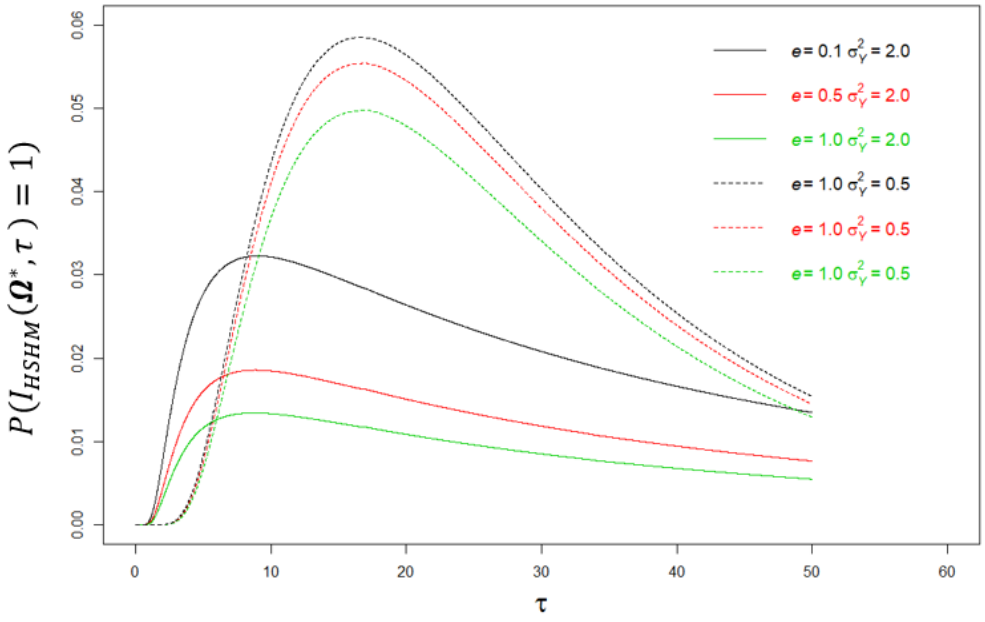

Figure 5. Dependence of $P(I_{HSHM}(\boldsymbol{\Omega}^*, \tau) = 1)$ on (τ) and on anisotropy ratio e. Solid and dashed lines represent, respectively, the probabilities for large $(\sigma_Y^2 = 2.0)$ and small $(\sigma_Y^2 = 0.5)$ variance of the log-hydraulic conductivity.

The discussion here (accompanying Figure 5) focuses on the impact of the anisotropy ratio in the correlation structure (e, defined above) on the ~~HSHM probabilities.~~probability of triggering HSHMs. The anisotropy ratio, e, provides an indication about the persistence of the log-conductivity (Y) in the ~~various~~principal directions. The spatial correlation model used here for demonstration is that of axis-symmetry, which is common to sedimentary formations

~~(Dagan, 1989; Rubin, 2003), with e providing the ratio between the persistence of Y in the vertical (x_3)~~(Dagan, 1989; Rubin, 2003), with e providing the ratio between the persistence of Y in the vertical (x_3) direction, represented by I_{YV}, and the ones on the horizontal plane ($x_1 - x_2$), represented by I_{YH}. In unconsolidated sedimentary formations, I_{YV} is typically smaller than I_{YH} by as much as one order of magnitude, due to the different time scales of the depositional process taking place in the horizontal and vertical directions, which leads to thin and elongated lithofacies and consequently to a much smaller persistence of Y values in normal to the horizontal plane (Miall, 1985, 1988; Ritzi et al., 2004).

Figure 5 compares ~~$\prec I_{HSHM} P(I_{HSHM}(\boldsymbol{\Omega}^*, \tau) \succ = 1)$~~ between formations defined by different anisotropy ratios and different σ_Y^2. It shows that we have two factors to consider when explaining the differences in ~~$\preccurlyeq I_{HSHM} P(I_{HSHM}(\boldsymbol{\Omega}^*, \tau) = 1). (\boldsymbol{\Omega}^*, \tau) \succ.$~~ First factor, as discussed earlier, is the ~~expansion in~~widening of the ~~range of~~ probability distribution (direct consequence of the widening of the travel times distribution) due to increase in σ_Y^2. With larger variance, we observe higher probabilities for departure of the travel times away from the average. The anisotropy ratio e adds a compounding factor. To understand its effect, we should recall the analyses of lateral displacement variances of solute particles moving in heterogeneous formations (cf., ~~Dagan, 1989, and Eq.~~Dagan, 1989, and Eq. A4 to A6 here), showing that smaller e leads to smaller lateral (both vertical and horizontal) displacement variances, implying smaller probabilities for lateral departures from the mean flow trajectory. Smaller e limits lateral spreads, and increase the probability of particle to enter $\boldsymbol{\Omega}^*$, sooner or later, and to trigger HSHM. The effect could also be viewed as a channeling effect of sorts: smaller e implies Y blocks of small aspect ratio (i.e., long but thin elements), which provide fast tracks for particles when defined by high Y values, while blocking lateral spreads when defined by low Y values.

~~There are a few additional things to note here for completeness. First, $\boldsymbol{\Omega}^*$ in the present analysis is located downstream from the source, along with the mean trajectory of the solute displacement. We expect different results in situations where $\boldsymbol{\Omega}^*$ is positioned at an offset with respect to the mean flow direction. Second, we note that the analytical models used to compute the displacement statistics are formally limited to smaller variance ($\sigma_Y^2 < 1$), although they are shown to provide good approximations for large variances (Bellin et al., 1992).Third, the stochastic formulation provides the theoretical and computational formalism for conditioning the probabilities on in situ measurements (Copty et al., 1993; Ezzedine and Rubin, 1996; Hubbard et al., 1997; Maxwell et al., 1999; Rubin, 1991a; Rubin et al., 1992; Rubin and Dagan, 1992) as well as on information borrowed from similar sites (Li et al., 2018; Cucchi et al., 2019).~~

In additional notes: first, $\boldsymbol{\Omega}^*$ is known in the present analysis is located downstream from the source, along with the mean trajectory of the solute displacement. We expect different results in situations where $\boldsymbol{\Omega}^*$ is positioned at an offset with respect to the mean flow direction, or when its position is unknown. In both cases we expect a reduction of the probability of triggering a HSHM. Relevant of our discussion is that the proposed probabilistic framework can address the case of unknown position for $\boldsymbol{\Omega}^*$ as well. Second, we note that the analytical models used to compute the displacement statistics are formally limited to small variance of the log-conductivity ($\sigma_Y^2 < 1$), although they are shown to provide good approximations for large variances (Bellin et al., 1992; Salandin and Fiorotto, 1998). Third, the stochastic formulation provides the theoretical and computational formalism for conditioning the

probabilities on in-situ measurements (Ezzedine and Rubin, 1996; Rubin and Dagan, 1992) as well as on information borrowed from similar sites (Li et al., 2018; Cucchi et al., 2019).

5 Discussion and Summary

In this study, we developed a general stochastic framework ~~that could be used to characterize~~for characterizing the spatiotemporal distribution of environmental Hot Spots Hot Moments (HSHMs~~), with groundwater applications.~~). The stochastic formulation is built around the following principles:

- The HSHMs are defined as random variables and the goal is to derive their stochastic distribution in terms of the relevant processes and attributes.
- HSHMs processes cover the dynamic components of the HSHMs. An example could be the transport of solutes and reactants. HSHMs attributes refer to the static components of the HSHMs, e.g., in situations related to the nitrogen ~~cycles~~cycle, attributes could represent pyrite ~~concentrations~~concentration or naturally-reducing zones. HSHMs could be defined through the confluence of a variety of contributors, both static and dynamic.
- The processes and attributes are modeled as stochastic processes and random variables, respectively, based on the underlying physics.
- The static contributors are modeled stochastically using geostatistical space random functions.
- The dynamic contributors are modeled stochastically using probability distribution functions derived from the underlying mathematical-physical models.
- Several HSHMs categories are defined, based on the contributing factors, as follows: HSHMs defined by dynamic contributors only, HSHMs defined by static contributors, and most commonly, HSHMs requiring the coupling of static and dynamic contributors. The HSHMs stochastic formulations are expressed in terms of the stochastic formulations of the relevant contributors.
- We provided a detailed review of multiple HSHMs and showed how they relate to our definitions.

The framework we proposed in this study is advantageous in that it allows to calculate the uncertainty associated with HSHMs based on the uncertainty associated with its contributors. Additionally, it provides a formalism, well established by Bayesian theory, for conditioning the HSHM probabilities on *in-situ* measurements as well as on information borrowed from geologically and otherwise similar sites.

We demonstrated our proposed approach through applications in the area of subsurface transport and hydrogeology, focusing on the impacts of subsurface heterogeneity on HSHMs. We analyzed, quantitatively, how subsurface heterogeneity of the conductivity field control the HSHM statistics, for example, the time expected for the probability of the HSHM to occur to reach a-priori set thresholds or time to peak probability.

Lastly, as mentioned both here and in previous studies, statistical methods for quantifying the occurrences of HSHMs and the associated uncertainties are needed to advance our understanding of the mechanisms that cause HSHMs, as well as to enhance our ability to predict HSHMs and manage their consequences.

Acknowledgments

We gratefully acknowledge the Jane Lewis Fellowship Committee of the University of California, Berkeley, and the Earth and Environmental Science Division at Lawrence Berkeley National Laboratory for their generous support through fellowships awarded to the first author. The second author's work is supported by the Office of Science, Office of Advanced Scientific Computing, as part of the project "Deduce: Distributed Dynamic Data Analytics Infrastructure for Collaborative Environments" under contract no. DE-AC02-05CH11231. The third author acknowledges funding from the Italian Ministry of Education, University and Research (MIUR) in the frame of the Departments of Excellence Initiative 2018—2022 granted to DICAM of the University of Trento. As this study focused on theory development, data were not used, nor created for this research. All the information needed for evaluating and checking the results is provided in the paper.

References

Andrews, D. M., Lin, H., Zhu, Q., Jin, L. and Brantley, S. L.: Hot spots and hot moments of dissolved organic carbon export and soil organic carbon storage in the shale hills catchment, Vadose Zo. J., 10(3), 943–954, doi:10.2136/vzj2010.0149, 2011.

Arora, B., Dwivedi, D., Hubbard, S. S., Steefel, C. I. and Williams, K. H.: Identifying geochemical hot moments and their controls on a contaminated river floodplain system using wavelet and entropy approaches, Environ. Model. Softw., 85, 27–41, doi:10.1016/j.envsoft.2016.08.005, 2016a.

Arora, B., Spycher, N. F., Steefel, C. I., Molins, S., Bill, M., Conrad, M. E., Dong, W., Faybishenko, B., Tokunaga, T. K., Wan, J., Williams, K. H. and Yabusaki, S. B.: Influence of hydrological, biogeochemical and temperature transients on subsurface carbon fluxes in a flood plain environment, Biogeochemistry, 127(2–3), 367–396, doi:10.1007/s10533-016-0186-8, 2016b.

Arora, B., Briggs, M. A., Zarnetske, J., Stegen, J., Gomez-Valez, J., Dwivedi, D. and Steefel, C.: Hot Spots and Hot Moments in the Critical Zone: Identification of and Incorporation into Reactive Transport Models, edited by A. Wymore, W. Yang, W. Silver, B. McDowell, and J. Chorover, Biogeochemistry of the Critical Zone, Springer Nature, Accepted., 2020.

Bao, C., Wu, H., Li, L., Newcomer, D., Long, P. E. and Williams, K. H.: Uranium bioreduction rates across scales: Biogeochemical hot moments and hot spots during a biostimulation experiment at Rifle, Colorado, Environ. Sci. Technol., doi:10.1021/es501060d, 2014.

Baum, R., Bartram, J. and Hrudey, S.: The Flint Water Crisis Confirms That U.S. Drinking Water Needs Improved Risk Management, Environ. Sci. Technol., 50(11), 5436–5437, doi:10.1021/acs.est.6b02238, 2016.

Bellin, A. and Rubin, Y.: On the use of peak concentration arrival times for the inference of hydrogeological parameters, Water Resour. Res., doi:10.1029/2003WR002179, 2004.

Bellin, A., Salandin, P. and Rinaldo, A.: Simulation of dispersion in heterogeneous porous formations: Statistics, first-order theories, convergence of computations, Water Resour. Res., doi:10.1029/92WR00578, 1992.

Bellin, A., Rubin, Y. and Rinaldo, A.: Eulerian Lagrangian approach for modeling of flow and transport in heterogeneous geological formations, Water Resour. Res., 30(11), 2913–2924, doi:10.1029/94WR01489, 1994.

Bernhardt, E. S., Blaszczak, J. R., Ficken, C. D., Fork, M. L., Kaiser, K. E. and Seybold, E. C.: Control Points in

Ecosystems: Moving Beyond the Hot Spot Hot Moment Concept, Ecosystems, 20(4), 665–682, doi:10.1007/s10021-016-0103-y, 2017.

Beven, K. J. and Kirkby, M. J.: A physically based, variable contributing area model of basin hydrology, Hydrol. Sci. Bull., doi:10.1080/02626667909491834, 1979.

Bundt, M., Widmer, F., Pesaro, M., Zeyer, J. and Blaser, P.: Preferential flow paths: Biological "hot spots" in soils, Soil Biol. Biochem., 33(6), 729–738, doi:10.1016/S0038-0717(00)00218-2, 2001.

Copty, N., Rubin, Y. and Mavko, G.: Geophysical-hydrological identification of field permeabilities through Bayesian updating, Water Resour. Res., 29(8), 2813–2825, doi:10.1029/93WR00745, 1993.

Cvetkovic, V., Shapiro, A. M. and Dagan, G.: A solute-flux approach to transport in heterogeneous formations: 2. Uncertainty analysis, Water Resour. Res., 28(5), 1377–1388, doi:10.1029/91WR03085, 1992.

Cvetkovic, V. D. and Shapiro, A. M.: Mass arrival of sorptive solute in heterogeneous porous media, Water Resour. Res., 26(9), 2057–2067, doi:10.1029/WR026i009p02057, 1990.

Dagan, G.: Solute transport in heterogeneous porous formations, J. Fluid Mech., 145(2), 151–177, doi:10.1017/S0022112084002858, 1984.

Dagan, G.: Flow and Transport in Porous Formations., Springer-Verlag, Berlin., 1989.

Dagan, G. and Nguyen, V.: A comparison of travel-time and concentration approaches to modeling transport by groundwater, J. Contam. Hydrol., 4(1), 79–91, doi:10.1016/0169-7722(89)90027-2, 1989.

Dagan, G. and Rubin, Y.: Conditional estimation of solute travel time in heterogeneous formations: Impact of transmissivity measurements, Water Resour. Res., 28(4), 1033–1040 [online] Available from: http://www.agu.org/pubs/crossref/1992.../91WR02759.shtml, 1992.

Destouni, G. and Cvetkovic, V.: Field scale mass arrival of sorptive solute into the groundwater, Water Resour. Res., 27(6), 1315–1325, doi:10.1029/91WR00182, 1991.

Duncan, J. M., Groffman, P. M. and Band, L. E.: Towards closing the watershed nitrogen budget: Spatial and temporal scaling of denitrification, J. Geophys. Res. Biogeosciences, 118(3), 1105–1119, doi:10.1002/jgrg.20090, 2013a.

Duncan, J. M., Groffman, P. M. and Band, L. E.: Towards closing the watershed nitrogen budget: Spatial and temporal scaling of denitrification, J. Geophys. Res. Biogeosciences, 118(3), 1105–1119, doi:10.1002/jgrg.20090, 2013b.

Dwivedi, D.: Hot Spots and Hot Moments of Nitrogen in a Riparian Corridor, Water Resour. Res., 1–43, doi:10.1002/2017WR022346, 2017.

Ezzedine, S. and Rubin, Y.: A geostatistical approach to the conditional estimation of spatially distributed solute concentration and notes on the use of tracer data in the inverse problem, Water Resour. Res., doi:10.1029/95WR02285, 1996.

Fiori, A. and Jankovic, I.: On Preferential Flow, Channeling and Connectivity in Heterogeneous Porous Formations, Math. Geosci., 44(2), 133–145, doi:10.1007/s11004-011-9365-2, 2012.

Frei, S., Knorr, K. H., Peiffer, S. and Fleckenstein, J. H.: Surface micro-topography causes hot spots of biogeochemical activity in wetland systems: A virtual modeling experiment, J. Geophys. Res. Biogeosciences, 117(4), 1–18, doi:10.1029/2012JG002012, 2012.

Gu, C., Anderson, W. and Maggi, F.: Riparian biogeochemical hot moments induced by stream fluctuations, Water

Resour. Res., 48(9), 1–17, doi:10.1029/2011WR011720, 2012.

Harken, B., Chang, C. F., Dietrich, P., Kalbacher, T. and Rubin, Y.: Hydrogeological Modeling and Water Resources Management: Improving the Link Between Data, Prediction, and Decision Making, Water Resour. Res., doi:10.1029/2019WR025227, 2019.

Harms, T. K. and Grimm, N. B.: Hot spots and hot moments of carbon and nitrogen dynamics in a semiarid riparian zone, J. Geophys. Res. Biogeosciences, 113(G1), n/a–n/a, doi:10.1029/2007JG000588, 2008.

Henri, C. V., Fernàndez-Garcia, D. and de Barros, F. P. J.: Probabilistic human health risk assessment of degradation-related chemical mixtures in heterogeneous aquifers: Risk statistics, hot spots, and preferential channels, Water Resour. Res., 51(6), 4086–4108, doi:10.1002/2014WR016717, 2015.

Hill, A. R., Devito, K. J. and Campagnolo, S.: Subsurface Denitrification in a Forest Riparian Zone : Interactions between Hydrology and Supplies of Nitrate and Organic Carbon Author (s): Alan R . Hill , Kevin J . Devito , S . Campagnolo and K . Sanmugadas Published by : Springer Stable URL : http:/, , 51(2), 193–223, 2000.

Hubbard, S. S., Rubin, Y. and Majer, E.: Ground-penetrating-radar-assisted saturation and permeability estimation in bimodal systems, Water Resour. Res., 33(5), 971–990, doi:10.1029/96WR03979, 1997.

Hubbard, S. S., Williams, K. H., Agarwal, D., Banfield, J., Beller, H., Bouskill, N., Brodie, E., Carroll, R., Dafflon, B., Dwivedi, D., Falco, N., Faybishenko, B., Maxwell, R., Nico, P., Steefel, C., Steltzer, H., Tokunaga, T., Tran, P. A., Wainwright, H. and Varadharajan, C.: The East River, Colorado, Watershed: A Mountainous Community Testbed for Improving Predictive Understanding of Multiscale Hydrological–Biogeochemical Dynamics, Vadose Zo. J., 17(1), 0, doi:10.2136/vzj2018.03.0061, 2018.

Kamidaira, Y., Uchiyama, Y., Kawamura, H., Kobayashi, T. and Furuno, A.: Submesoscale Mixing on Initial Dilution of Radionuclides Released From the Fukushima Daiichi Nuclear Power Plant, J. Geophys. Res. Ocean., 123(4), 2808–2828, doi:10.1002/2017JC013359, 2018.

Li, L., Steefel, C. I., Kowalsky, M. B., Englert, A. and Hubbard, S. S.: Effects of physical and geochemical heterogeneities on mineral transformation and biomass accumulation during biostimulation experiments at Rifle, Colorado, J. Contam. Hydrol., 112(1–4), 45–63, doi:10.1016/j.jconhyd.2009.10.006, 2010.

Loschko, M., Wochling, T., Rudolph, D. L. and Cirpka, O. A.: Cumulative relative reactivity: A concept for modeling aquifer-scale reactive transport, Water Resour. Res., 52(10), 8117–8137, doi:10.1002/2016WR019080, 2016.

Maxwell, R. M., Kastenberg, W. E. and Rubin, Y.: A methodology to integrate site characterization information into groundwater-driven health risk assessment, Water Resour. Res., doi:10.1029/1999WR900103, 1999.

McClain, M. E., Boyer, E. W., Dent, C. L., Gergel, S. E., Grimm, N. B., Groffman, P. M., Hart, S. C., Harvey, J. W., Johnston, C. A., Mayorga, E., McDowell, W. H. and Pinay, G.: Biogeochemical Hot Spots and Hot Moments at the Interface of Terrestrial and Aquatic Ecosystems, Ecosystems, 6(4), 301–312, doi:10.1007/s10021-003-0161-9, 2003.

Miall, A. D.: Architectural-element analysis: A new method of facies analysis applied to fluvial deposits, Earth Sci. Rev., doi:10.1016/0012-8252(85)90001-7, 1985.

Miall, A. D.: Facies Architecture in Clastic Sedimentary Basins., 1988.

Mitchell, C. P. J., Branfireun, B. A. and Kolka, R. K.: Spatial characteristics of net methylmercury production hot spots in peatlands, Environ. Sci. Technol., 42(4), 1010–1016, doi:10.1021/es0704986, 2008.

Moreno, L. and Tsang, C. F: Flow channeling in strongly heterogeneous porous media: A numerical study, Water Resour. Res., doi:10.1029/93WR02978, 1994.

Morino, Y., Ohara, T. and Nishizawa, M.: Atmospheric behavior, deposition, and budget of radioactive materials from the Fukushima Daiichi nuclear power plant in March 2011, Geophys. Res. Lett., 38(17), 1–7, doi:10.1029/2011GL048689, 2011.

Ritzi, R. W., Dai, Z., Dominic, D. F. and Rubin, Y. N.: Spatial correlation of permeability in cross-stratified sediment with hierarchical architecture, Water Resour. Res., doi:10.1029/2003WR002420, 2004.

Rubin, Y.: Prediction of tracer plume migration in disordered porous media by the method of conditional probabilities, Water Resour. Res., doi:10.1029/91WR00094, 1991a.

Rubin, Y.: The Spatial and Temporal Moments of Tracer Concentration in Disordered Porous Media, Water Resour. Res., doi:10.1029/91WR01732, 1991b.

Rubin, Y.: Flow and Transport in Bimodal Heterogeneous Formations, Water Resour. Res., doi:10.1029/95WR01953, 1995.

Rubin, Y.: Applied Stochastic Hydrogeology, Oxford University Press, Oxford, UK., 2003.

Rubin, Y. and Dagan, G.: Conditional estimation of solute travel time in heterogeneous formations: Impact of transmissivity measurements, Water Resour. Res., doi:10.1029/91WR02759, 1992.

Rubin, Y. and Journel, A. G.: Simulation of non-Gaussian space random functions for modeling transport in groundwater, Water Resour. Res., doi:10.1029/91WR00838, 1991.

Rubin, Y., Mavko, G. and Harris, J.: Mapping permeability in heterogeneous aquifers using hydrologic and seismic data, Water Resour. Res., doi:10.1029/92WR00154, 1992.

Rubin, Y., Cushey, M. A. and Bellin, A.: Modeling of transport in groundwater for environmental risk assessment, Stoch. Hydrol. Hydraul., doi:10.1007/BF01581390, 1994.

Sassen, D. S., Hubbard, S. S., Bea, S. A., Chen, J., Spycher, N. and Denham, M. E.: Reactive facies: An approach for parameterizing field-scale reactive transport models using geophysical methods, Water Resour. Res., 48(10), doi:10.1029/2011WR011047, 2012.

Showstack, R.: Fukushima Nuclear Accident Report Calls for More Focus on Threats From Extreme Events, Eos, Trans. Am. Geophys. Union, 95(31), 279–279, doi:10.1002/2014eo310003, 2014.

Shrestha, N. K. and Wang, J.: Current and future hot spots and hot moments of nitrous oxide emission in a cold climate river basin, Environ. Pollut., 239, 648–660, doi:10.1016/j.envpol.2018.04.068, 2018.

Sørensen, R., Zinko, U. and Seibert, J.: On the calculation of the topographic wetness index: Evaluation of different methods based on field observations, Hydrol. Earth Syst. Sci., doi:10.5194/hess-10-101-2006, 2006.

Teh, Y. A., Silver, W. L., Sonnentag, O., Detto, M., Kelly, M. and Baldocchi, D. D.: Large Greenhouse Gas Emissions from a Temperate Peatland Pasture, Ecosystems, 14(2), 311–325, doi:10.1007/s10021-011-9411-4, 2011.

USEPA: Risk Assessment Guidance for Superfund., 2001.

Vidon, P., Allan, C., Burns, D., Duval, T. P., Gurwick, N., Inamdar, S., Lowrance, R., Okay, J., Scott, D. and Sebestyen, S.: Hot spots and hot moments in riparian zones: Potential for improved water quality management, J. Am. Water Resour. Assoc., 46(2), 278–298, doi:10.1111/j.1752-1688.2010.00420.x, 2010.

~~Wainwright, H. M., Orozco, A. F., Bucker, M., Dafflon, B., Chen, J., Hubbard, S. S. and Williams, K. H.: Hierarchical Bayesian method for mapping biogeochemical hot spots using induced polarization imaging, Water Resour. Res., 51, 9127–9140, doi:10.1002/2014WR016259, 2015.~~

~~Wilson, A. and Rubin, Y.: Characterization of aquifer heterogeneity using indicator variables for solute concentrations, Water Resour. Res., 38(12), 19–1–19–12, doi:10.1029/2000wr000116, 2002.~~

Appendix

A1. Equations for the displacement pdf

Assuming steady, uniform in the average flow, with mild heterogeneity of the log-hydraulic conductivity field with Gaussian displacement, the ~~displacement~~ pdf ~~in~~of the longitudinal ~~direction~~ (x_1~~)~~, Figure 3) displacement of a solute particle starting at time $t_0 = 0$, at $\boldsymbol{x}_0$ =(0,0,0) is given by the following equation ~~(Dagan and Nguyen, 1989; Dagan and Rubin, 1992)~~(Dagan and Nguyen, 1989; Dagan and Rubin, 1992):

$$f_{X_1(t^*)}(x_1) = \frac{1}{\sqrt{2\pi X_{11}(t^*)}} \exp\left[-\frac{1}{2}\frac{(x_1 - Ut^*)^2}{X_{11}(t^*)}\right]. \quad \text{(A1)}$$

Additionally, the displacement pdf in the transverse directions (x_2 and x_3) is given by

$$f_{X_i(t^*)}(x_i) = \frac{1}{\sqrt{2\pi X_{ii}(t^*)}} \exp\left[-\frac{1}{2}\frac{x_i^2}{X_{ii}(t^*)}\right], i = 2,3. \quad \text{(A2)}$$

A2. Equations for displacement variances under anisotropic conditions

~~Dagan (1984) developed a solution for the displacement variances for an exponential and axisymmetric~~Dagan (1984) developed a solution of the displacement variances $X_{ii}, i = 1,2,3$ for an exponential and axisymmetric logconductivity covariance function:

$$C_Y(\boldsymbol{r}) = \langle (Y(\boldsymbol{x}) - \langle Y \rangle)\,(Y(\boldsymbol{x}+\boldsymbol{r}) - \langle Y \rangle) \rangle = \sigma_Y^2 \exp\left[-\sqrt{\frac{r_1^2+r_2^2}{I_{Yh}^2} + \frac{r_3^2}{I_{Yv}^2}}\right], \quad \text{(A3)}$$

$$X_{11} = \sigma_Y^2 I_Y^2 \{2t^* + 2[\exp(-t^*) - 1] + 8e \int_0^\infty [\bar{J}_0(Kt^*) - 1] \cdot \left[\frac{1}{(1+K^2-\mathrm{e}^2K^2)^2} - \frac{\mathrm{e}K}{(1+K^2-\mathrm{e}^2K^2)^2(1+K^2)^{0.5}} - \frac{\mathrm{e}K}{2(1+K^2-\mathrm{e}^2K^2)(1+K^2)^{1.5}}\right] dK$$
$$-2\mathrm{e}\int_0^\infty \left[\bar{J}_0(Kt^*) - \frac{\bar{J}_1(Kt^*)}{Kt^*} - \frac{1}{2}\right] \cdot \left[\frac{\mathrm{e}^3K^3(\mathrm{e}^2K^2 - 5 - 5K^2)}{(\mathrm{e}^2K^2 - 1 - K^2)^3(1+K^2)^{1.5}} + \frac{1+K^2-5\mathrm{e}^2K^2}{(1+K^2-\mathrm{e}^2K^2)^3}\right] dK\}, \quad (A4)$$

$$X_{22} = -2\mathrm{e}\sigma_Y^2 I_Y^2 \cdot \int_0^\infty \left[\frac{\bar{J}_1(Kt^*)}{t^*} - \frac{K}{2}\right] \left[\frac{\mathrm{e}^3K^2(\mathrm{e}^2K^2 - 5K^2 - 5)}{(\mathrm{e}^2K^2 - 1 - K^2)^3(1+K^2)^{1.5}} + \frac{1+K^2-5\mathrm{e}^2K^2}{K(1+K^2-\mathrm{e}^2K^2)}\right] dK, \quad \text{(A5)}$$

$$X_{33} = -4\mathrm{e}\sigma_Y^2 I_Y^2 \int_0^\infty [\bar{J}_0(Kt^*) - 1]$$

$$\cdot\left\{\frac{1}{(e^2K^2-1-K^2)^2}\left[\frac{1}{2}+\frac{2e^2K^2}{1+K^2-e^2K^2}+\frac{eK(e^2K^2+3+3K^2)}{2(e^2K^2-1-K^2)(1+K^2)^{0.5}}\right]\right\}dK. \quad \text{(A6)}$$

where $\boldsymbol{r}$ is the two-point separation distance and $\langle Y\rangle$ the ensemble mean of the log-conductivity $Y=\ln K$. $\overline{J_0}$ and $\overline{J_1}$ are, respectively, the zero and first order of the first kind Bessel functions.

A3. Equations for displacement variances under isotropic conditions

~~Dagan (1984)~~Dagan (1984) provided analytical solutions for ~~longitude~~longitudinal and transverse displacement variances. This is a special case for the anisotropic case with $e=1$.The solutions are as follows:

$$X_{11}=\sigma_Y^2 I_Y^2\left\{2t^*-2\cdot\left[\frac{8}{3}-\frac{4}{t^*}+\frac{8}{t^{*3}}-\frac{8}{t^{*2}}\left(1+\frac{1}{t^*}\right)\exp(-t^*)\right]\right\}. \quad \text{(A7)}$$

$$X_{22}=X_{33}=2\sigma_Y^2 I_Y^2\left[\frac{1}{3}-\frac{1}{t^*}+\frac{4}{t^{*3}}-\left(\frac{4}{t^{*3}}+\frac{4}{t^{*2}}+\frac{1}{t^*}\right)\exp(-t^*)\right]. \quad \text{(A8)}$$

A4. Indicator formulation for complex concentration thresholds

When considering local dispersion, or in case of a reactive tracer, the condition that the particle is inside the volume $\boldsymbol{\Omega}^*$ does not suffice to define the dynamic indicator and a concentration threshold C_{th} should be introduced:

$$I_d(\boldsymbol{\Omega}^*,t^*)=\begin{cases}1, & if\ \boldsymbol{X}(t^*;\boldsymbol{x}_0,t_0)\subseteq\boldsymbol{\Omega}^*\ and\ C(\boldsymbol{X},t^*)>C_{th}\\ 0, & otherwise\end{cases}. \quad \text{(A9)}$$

In the absence of local dispersion and for a reactive solute decaying at a (spatially) constant rate k, the ensemble mean assumes the following expression (Cvetkovic and Shapiro, 1990):

$$P(I_d(\boldsymbol{\Omega}^*,t^*)=1)=<I_d(\boldsymbol{\Omega}^*,t^*)>=\left\{1-H\left[t^*-\frac{1}{k}\ln\left(\frac{C_0}{C_{th}}\right)\right]\right\}\int_{\Omega^*}f_{\boldsymbol{X}(t^*)}(\boldsymbol{a}|\boldsymbol{x}_0,t_0)d\boldsymbol{a}, \quad \text{(A10)}$$

where C_0 is the initial concentration and $H[\cdot]$ is the Heaviside step function. The ensemble mean (Eq. A10) is the product of the probability that the particle assumes a concentration larger than the threshold at t^* (given that reaction rate k is constant, this probability is either 0 or 1) and the probability that at the same time t^* the particle is within the hot spot $\boldsymbol{\Omega}^*$. In other words, Eq. (A10) expresses the fact that a particle inside $\boldsymbol{\Omega}^*$ contributes to the hot moment only if its concentration is greater than the threshold, and this occurs for $t^*<\frac{1}{k}\ln\left(\frac{C_0}{C_{th}}\right)$. Eq. (A10) can be generalized to the cases of instantaneous injection into a source of volume V_0, as discussed before for the non-reactive case. For other complex situations, such as that in which k is spatially variable and complex reaction networks, the ensemble mean of the indicators can be addressed by Eq. (16) in a Monte Carlo framework.

A5. Indicator formulation for hot moment durations

As hot moments can persist over short time perids, estimating the corresponding probabilities for any given time interval becomes also very importatnt. The probability that the hot moment persists over the interval $[t_1,t_2]$ at $\boldsymbol{\Omega}^*$ can be formally computed as follows:

$$<I_d(\boldsymbol{\Omega}^*,t_1,t_2)>=P(t_1,\boldsymbol{\Omega}^*)P(t_2|t_1,\boldsymbol{\Omega}^*), \quad \text{(A11)}$$

where $P(t_1,\boldsymbol{\Omega}^*)$ is the probability that the particle is inside $\boldsymbol{\Omega}^*$ at time $t^*=t_1$ and $P(t_2|t_1,\boldsymbol{\Omega}^*)$ is the probability that the particle is still inside $\boldsymbol{\Omega}^*$ at time $t^*=t_2$, provided that at time t_1, it was also inside $\boldsymbol{\Omega}^*$. If the particle exits $\boldsymbol{\Omega}^*$

during interval $[t_1, t_2]$, this time interval will not be qualified as hot moment; and thus the probability computation needs to ensure the particle stays within $\boldsymbol{\Omega}^*$ during the entire time interval.

Under the First-Order Approximation (FOA) (see e.g., Dagan, 1989; Gelhar 1993; Rubin, 2003), the pdf of the particle displacement is normal with mean $< \boldsymbol{X}(t^*; \boldsymbol{x_0}, t_0) >$ and auto-covariance tensor of the residual displacements $\boldsymbol{X}'(t^*) = \boldsymbol{X}(t^*) - \langle \boldsymbol{X}(t^*) \rangle$ defined by $\boldsymbol{X}_{ij}(t^*; \boldsymbol{x}_0, t_0) = \langle \boldsymbol{X}'_i(t^*; \boldsymbol{x}_0, t_0) \boldsymbol{X}'_j(t^*; \boldsymbol{x}_0, t_0) \rangle,\ i, j = 1, 2, 3.$ For simplicity in the following, we assume $\boldsymbol{x}_0 = 0\ and\ t_0 = 0$. Under these assumptions,

$$< I_d(\boldsymbol{\Omega}^*, t_1, t_2) >= \int_{\boldsymbol{\Omega}^*} \int_{\boldsymbol{\Omega}^*} f_{\boldsymbol{X}(t_1)}(\boldsymbol{a}) f^c_{\boldsymbol{X}(t_2)}(\boldsymbol{b} | \boldsymbol{X}(t_1) = \boldsymbol{a})\, d\boldsymbol{b}\, d\boldsymbol{a}, \tag{A12}$$

where the conditional pdf $f^c_{\boldsymbol{X}(t_2)}(\boldsymbol{b} | \boldsymbol{X}(t_1) = \boldsymbol{a})$ is multi-normally distributed with conditional mean and variance tensor given by

$$\langle \boldsymbol{X}(t_2) | \boldsymbol{X}(t_1) = \boldsymbol{a}) \rangle = < \boldsymbol{X}(t_2) > + Cov[\boldsymbol{X}'(t_2), \boldsymbol{X}'(t_1)] \cdot Var[\boldsymbol{X}'(t_1)]^{-1} \cdot (\boldsymbol{a} - < \boldsymbol{X}(t_1) >), \tag{A13}$$

and

$$\boldsymbol{\sigma}(t_1, t_2) = Var[\boldsymbol{X}'(t_2)] - Cov[\boldsymbol{X}'(t_2), \boldsymbol{X}'(t_1)] \cdot Var[\boldsymbol{X}'(t_1)]^{-1} \cdot Cov[\boldsymbol{X}'(t_1), \boldsymbol{X}'(t_2)], \tag{A14}$$

respectively, which further yields the following,

$$f^c_{\boldsymbol{X}(t_2)}(\boldsymbol{b} | \boldsymbol{X}(t_1) = \boldsymbol{a}) = \exp\left[-\frac{1}{2} [\boldsymbol{b} - \langle \boldsymbol{X}(t_2) | \boldsymbol{X}(t_1) = \boldsymbol{a}) \rangle]^T \cdot \boldsymbol{\sigma}(t_1, t_2)^{-1} \cdot [\boldsymbol{b} - \langle \boldsymbol{X}(t_2) | \boldsymbol{X}(t_1) = \boldsymbol{a}) \rangle] \right] \cdot \{8\, \pi^3 \cdot |\boldsymbol{\sigma}(t_1, t_2)|\}^{-\frac{1}{2}}, \tag{A15}$$

where $|\cdot|$ indicates the determinant, exp is the exponential function and the exponent T indicates the transpose of the vector.

In Eq. (A13) and (A14), $\boldsymbol{X}'(t^*) = \boldsymbol{X}(t^*) - \langle \boldsymbol{X}(t^*) \rangle$ stands for the departure of the particle's displacement with respect to the ensemble mean trajectory, and $Var[\boldsymbol{X}]^{-1}$ is the auto-covariance tensor of the residual displacement whose elements are defined above. Similarly, $Cov[\boldsymbol{X}'(t_1), \boldsymbol{X}'(t_2)]$ is the covariance tensor of residual displacement which elements are: $\boldsymbol{X}_{ij}(t_1, t_2; \boldsymbol{x_0}, t_0) = \langle X'_i(t_1)\, X'_j(t_2) \rangle, i, j = 1, 2, 3$. Note that in the general three-dimensional case $\langle \boldsymbol{X}(t_2) | \boldsymbol{X}(t_1) = \boldsymbol{a}) \rangle$ is a three-dimensional vector and $\boldsymbol{\sigma}(t_1, t_2)$ is a 3×3 second-order tensor.

For $t_2 \to t_1$, $f^c_{\boldsymbol{X}(t_2)}[\boldsymbol{b} | \boldsymbol{X}(t_1) = \boldsymbol{a}] \to \delta(\boldsymbol{b} - \boldsymbol{a})$, where $\delta(\cdot)$ is the Dirac Delta, such that $P(t_2 | t_1, \boldsymbol{\Omega}^*) \to 1$. On the other hand, for $t_2 \gg t_1$, $Cov[\boldsymbol{X}'(t_1), \boldsymbol{X}'(t_2)] \to 0$ and $P(t_2 | t_1, \boldsymbol{\Omega}^*) \to P(t_2, \boldsymbol{\Omega}^*)$ the marginal probability that the particle is within $\boldsymbol{\Omega}^*$ at time $t^* = t_2$. Eq. (A12) to (A15) are obtained under the FOA approximation and assuming that the particle can enter $\boldsymbol{\Omega}^*$ only once. Such assumption is needed to obtain analytical solutions and is reasonable for situations with small to mild subsurface heterogeneity (e.g., $\sigma_Y^2 \leq 1.6$), such as the cases presented in Bellin et al. (1992, 1994); Cvetkovic et al. (1992). In particular, FOA assumes small heterogeneity and under this assumption the particle trajectory deviates slightly from its ensemble mean, which is directed along the regional hydraulic head gradient. For a regular volume $\boldsymbol{\Omega}^*$, this reduces the probability of the particle entering more than once the hot spot. This probability reduces further if in horizontal and vertical transverse directions $\boldsymbol{\Omega}^*$ is much larger than the respective integral scales, because the probability of observing negative longitudinal velocity components (i.e., along the mean

flow field) is much smaller than in the transverse directions (Bellin et al., 1992) and vanishes as formation heterogeneity reduces.

If the hotspot $\boldsymbol{\Omega}^*$ is the volume confined between two planes at $x_1 - \frac{l_1}{2}$ and $x_1 + \frac{l_1}{2}$, with the other two dimensions much larger than the transverse horizontal and vertical integral scales: $l_2 \gg I_h$, $l_3 \gg I_v$, Eq. (A13) simplifies to:

$$< I_d(\boldsymbol{\Omega}^*, t_1, t_2) >= \int_{x_1-\frac{l_1}{2}}^{x_1+\frac{l_1}{2}} \int_{x_1-\frac{l_1}{2}}^{x_1+\frac{l_1}{2}} f_{X_1(t^*)}(a_1) f^c_{X_1(t^*)}(\, b_1 | X_1(t_1) = a_1)\, db_1\, da_1, \tag{A16}$$

where X_1 is the longitudinal component of the particle's trajectory and $f^c_{X_1(t^*)}$ is its conditional pdf, which is normal with conditional mean and variance given by

$$\mu[a_1] = \langle X_1(t_2) |\, X_1(t_1) = a_1) \rangle = < X_1(t_2) > + \frac{X_{11}(t_1, t_2)}{X_{11}(t_1)} (a_1 - < X_1(t_1) >), \tag{A17}$$

and

$$\sigma^2(t_1, t_2) = X_{11}(t_2) - \frac{X_{11}(t_1, t_2)^2}{X_{11}(t_1)}, \tag{A18}$$

respectively. Consequently, $f_{X^c(t^*)}$ in Eq. (A16) assumes the following form:

$$f^c_{X_1(t^*)}(b_1 | X_1(t_1) = a_1) = \frac{1}{\sqrt{2\,\pi\,\sigma(t_1, t_2)}} \exp\left[-\frac{1}{2}(b_1 - \mu[a_1])^2\, \sigma(t_1, t_2)^{-1}\right]. \tag{A19}$$

Substituting Eq. (A16) into Eq. (A19) allows us to compute $< I_d(\boldsymbol{\Omega}^*, t_1, t_2) >$. For situations where the FOA assumptions are not valid (e.g., large heterogeneity), Monte Carlo simulation framework is still applicable as alternative approach to construct the dynamics indicators (see Eq. 16).

References

Abbott, B. W., Baranov, V., Mendoza-Lera, C., Nikolakopoulou, M., Harjung, A., Kolbe, T., Balasubramanian, M. N., Vaessen, T. N., Ciocca, F., Campeau, A., Wallin, M. B., Romeijn, P., Antonelli, M., Gonçalves, J., Datry, T., Laverman, A. M., de Dreuzy, J. R., Hannah, D. M., Krause, S., Oldham, C. and Pinay, G.: Using multi-tracer inference to move beyond single-catchment ecohydrology, Earth-Science Rev., 160, 19–42, doi:10.1016/j.earscirev.2016.06.014, 2016.

Akaike, H.: A New Look at the Statistical Model Identification, IEEE Trans. Automat. Contr., doi:10.1109/TAC.1974.1100705, 1974.

Andrews, D. M., Lin, H., Zhu, Q., Jin, L. and Brantley, S. L.: Hot spots and hot moments of dissolved organic carbon export and soil organic carbon storage in the shale hills catchment, Vadose Zo. J., 10(3), 943–954, doi:10.2136/vzj2010.0149, 2011.

Arora, B., Mohanty, B. P., McGuire, J. T. and Cozzarelli, I. M.: Temporal dynamics of biogeochemical processes at the Norman Landfill site, Water Resour. Res., 49(10), doi:10.1002/wrcr.20484, 2013.

Arora, B., Dwivedi, D., Hubbard, S. S., Steefel, C. I. and Williams, K. H.: Identifying geochemical hot moments and their controls on a contaminated river floodplain system using wavelet and entropy approaches, Environ. Model. Softw., 85, 27–41, doi:10.1016/j.envsoft.2016.08.005, 2016a.

Arora, B., Spycher, N. F., Steefel, C. I., Molins, S., Bill, M., Conrad, M. E., Dong, W., Faybishenko, B., Tokunaga, T. K., Wan, J., Williams, K. H. and Yabusaki, S. B.: Influence of hydrological, biogeochemical and temperature transients on subsurface carbon fluxes in a flood plain environment, Biogeochemistry, 127(2–3), 367–396, doi:10.1007/s10533-016-0186-8, 2016b.

Arora, B., Wainwright, H. M., Dwivedi, D., Vaughn, L. J. S., Curtis, J. B., Torn, M. S., Dafflon, B. and Hubbard, S. S.: Evaluating temporal controls on greenhouse gas (GHG) fluxes in an Arctic tundra environment: An entropy-based approach, Sci. Total Environ., doi:10.1016/j.scitotenv.2018.08.251, 2019a.

Arora, B., Dwivedi, D., Faybishenko, B., Jana, R. B. and Wainwright, H. M.: Understanding and Predicting Vadose Zone Processes, Rev. Mineral. Geochemistry, 85(1), doi:10.2138/rmg.2019.85.10, 2019b.

Arora, B., Briggs, M. A., Zarnetske, J., Stegen, J., Gomez-Valez, J., Dwivedi, D. and Steefel, C.: Hot Spots and Hot Moments in the Critical Zone: Identification of and Incorporation into Reactive Transport Models, edited by A. Wymore, W. Yang, W. Silver, B. McDowell, and J. Chorover, Biogeochemistry of the Critical Zone, Springer-Nature, Accepted., 2021.

Bellin, A. and Rubin, Y.: On the use of peak concentration arrival times for the inference of hydrogeological parameters, Water Resour. Res., doi:10.1029/2003WR002179, 2004.

Bellin, A., Salandin, P. and Rinaldo, A.: Simulation of dispersion in heterogeneous porous formations: Statistics, first-order theories, convergence of computations, Water Resour. Res., doi:10.1029/92WR00578, 1992.

Bellin, A., Rubin, Y. and Rinaldo, A.: Eulerian-Lagrangian approach for modeling of flow and transport in heterogeneous geological formations, Water Resour. Res., 30(11), 2913–2924, doi:10.1029/94WR01489, 1994.

Bernhardt, E. S., Blaszczak, J. R., Ficken, C. D., Fork, M. L., Kaiser, K. E. and Seybold, E. C.: Control Points in Ecosystems: Moving Beyond the Hot Spot Hot Moment Concept, Ecosystems, 20(4), 665–682, doi:10.1007/s10021-016-0103-y, 2017.

Beven, K. J. and Kirkby, M. J.: A physically based, variable contributing area model of basin hydrology, Hydrol. Sci. Bull., doi:10.1080/02626667909491834, 1979.

Bundt, M., Widmer, F., Pesaro, M., Zeyer, J. and Blaser, P.: Preferential flow paths: Biological “hot spots” in soils, Soil Biol. Biochem., 33(6), 729–738, doi:10.1016/S0038-0717(00)00218-2, 2001.

Copty, N., Rubin, Y. and Mavko, G.: Geophysical-hydrological identification of field permeabilities through Bayesian updating, Water Resour. Res., 29(8), 2813–2825, doi:10.1029/93WR00745, 1993.

Cucchi, K., Heße, F., Kawa, N., Wang, C. and Rubin, Y.: Ex-situ priors: A Bayesian hierarchical framework for defining informative prior distributions in hydrogeology, Adv. Water Resour., doi:10.1016/j.advwatres.2019.02.003, 2019.

Cvetkovic, V., Shapiro, A. M. and Dagan, G.: A solute flux approach to transport in heterogeneous formations: 2. Uncertainty analysis, Water Resour. Res., 28(5), 1377–1388, doi:10.1029/91WR03085, 1992.

Cvetkovic, V. D. and Shapiro, A. M.: Mass arrival of sorptive solute in heterogeneous porous media, Water Resour. Res., 26(9), 2057–2067, doi:10.1029/WR026i009p02057, 1990.

Dagan, G.: Solute transport in heterogeneous porous formations, J. Fluid Mech., 145(2), 151–177, doi:10.1017/S0022112084002858, 1984.

Dagan, G.: Flow and Transport in Porous Formations., Springer Verlag, Berlin., 1989.

Dagan, G.: Transport in heterogeneous porous formations: Spatial moments, ergodicity, and effective dispersion, Water Resour. Res., 26(6), doi:10.1029/WR026i006p01281, 1990.

Dagan, G. and Nguyen, V.: A comparison of travel time and concentration approaches to modeling transport by groundwater, J. Contam. Hydrol., 4(1), 79–91, doi:10.1016/0169-7722(89)90027-2, 1989.

Dagan, G. and Rubin, Y.: Conditional estimation of solute travel time in heterogeneous formations: Impact of transmissivity measurements, Water Resour. Res., 28(4), 1033–1040 [online] Available from: http://www.agu.org/pubs/crossref/1992.../91WR02759.shtml, 1992.

Destouni, G. and Cvetkovic, V.: Field scale mass arrival of sorptive solute into the groundwater, Water Resour. Res., 27(6), 1315–1325, doi:10.1029/91WR00182, 1991.

Duncan, J. M., Groffman, P. M. and Band, L. E.: Towards closing the watershed nitrogen budget: Spatial and temporal scaling of denitrification, J. Geophys. Res. Biogeosciences, 118(3), 1105–1119, doi:10.1002/jgrg.20090, 2013a.

Duncan, J. M., Groffman, P. M. and Band, L. E.: Towards closing the watershed nitrogen budget: Spatial and temporal scaling of denitrification, J. Geophys. Res. Biogeosciences, 118(3), 1105–1119, doi:10.1002/jgrg.20090, 2013b.

Dwivedi, D.: Hot Spots and Hot Moments of Nitrogen in a Riparian Corridor, Water Resour. Res., 1–43, doi:10.1002/2017WR022346, 2017.

Ezzedine, S. and Rubin, Y.: A geostatistical approach to the conditional estimation of spatially distributed solute concentration and notes on the use of tracer data in the inverse problem, Water Resour. Res., doi:10.1029/95WR02285, 1996.

Fiori, A. and Jankovic, I.: On Preferential Flow, Channeling and Connectivity in Heterogeneous Porous Formations, Math. Geosci., 44(2), 133–145, doi:10.1007/s11004-011-9365-2, 2012.

Frei, S., Knorr, K. H., Peiffer, S. and Fleckenstein, J. H.: Surface micro-topography causes hot spots of biogeochemical activity in wetland systems: A virtual modeling experiment, J. Geophys. Res. Biogeosciences, 117(4), 1–18, doi:10.1029/2012JG002012, 2012.

Gu, C., Anderson, W. and Maggi, F.: Riparian biogeochemical hot moments induced by stream fluctuations, Water Resour. Res., 48(9), 1–17, doi:10.1029/2011WR011720, 2012.

Harms, T. K. and Grimm, N. B.: Hot spots and hot moments of carbon and nitrogen dynamics in a semiarid riparian zone, J. Geophys. Res. Biogeosciences, 113(1), 1–14, doi:10.1029/2007JG000588, 2008.

Henri, C. V., Fernàndez-Garcia, D. and de Barros, F. P. J.: Probabilistic human health risk assessment of degradation-related chemical mixtures in heterogeneous aquifers: Risk statistics, hot spots, and preferential channels, Water Resour. Res., 51(6), 4086–4108, doi:10.1002/2014WR016717, 2015.

Hill, A. R., Devito, K. J. and Campagnolo, S.: Subsurface Denitrification in a Forest Riparian Zone : Interactions between Hydrology and Supplies of Nitrate and Organic Carbon Author (s): Alan R . Hill , Kevin J . Devito , S . Campagnolo and K . Sanmugadas Published by : Springer Stable URL : http:/, , 51(2), 193–223, 2000.

Hubbard, S. S., Rubin, Y. and Majer, E.: Ground-penetrating-radar-assisted saturation and permeability estimation

in bimodal systems, Water Resour. Res., 33(5), 971–990, doi:10.1029/96WR03979, 1997.
Hubbard, S. S., Williams, K. H., Agarwal, D., Banfield, J., Beller, H., Bouskill, N., Brodie, E., Carroll, R., Dafflon, B., Dwivedi, D., Falco, N., Faybishenko, B., Maxwell, R., Nico, P., Steefel, C., Steltzer, H., Tokunaga, T., Tran, P. A., Wainwright, H. and Varadharajan, C.: The East River, Colorado, Watershed: A Mountainous Community Testbed for Improving Predictive Understanding of Multiscale Hydrological–Biogeochemical Dynamics, Vadose Zo. J., 17(1), 0, doi:10.2136/vzj2018.03.0061, 2018.
Li, X., Li, Y., Chang, C. F., Tan, B., Chen, Z., Sege, J., Wang, C. and Rubin, Y.: Stochastic, goal-oriented rapid impact modeling of uncertainty and environmental impacts in poorly-sampled sites using ex-situ priors, Adv. Water Resour., doi:10.1016/j.advwatres.2017.11.008, 2018.
Loschko, M., Woehling, T., Rudolph, D. L. and Cirpka, O. A.: Cumulative relative reactivity: A concept for modeling aquifer-scale reactive transport, Water Resour. Res., 52(10), 8117–8137, doi:10.1002/2016WR019080, 2016.
Maxwell, R. M., Kastenberg, W. E. and Rubin, Y.: A methodology to integrate site characterization information into groundwater-driven health risk assessment, Water Resour. Res., doi:10.1029/1999WR900103, 1999.
McClain, M. E., Boyer, E. W., Dent, C. L., Gergel, S. E., Grimm, N. B., Groffman, P. M., Hart, S. C., Harvey, J. W., Johnston, C. A., Mayorga, E., McDowell, W. H. and Pinay, G.: Biogeochemical Hot Spots and Hot Moments at the Interface of Terrestrial and Aquatic Ecosystems, Ecosystems, 6(4), 301–312, doi:10.1007/s10021-003-0161-9, 2003.
Miall, A. D.: Architectural-element analysis: A new method of facies analysis applied to fluvial deposits, Earth Sci. Rev., doi:10.1016/0012-8252(85)90001-7, 1985.
Miall, A. D.: Facies Architecture in Clastic Sedimentary Basins., 1988.
Mitchell, C. P. J., Branfireun, B. A. and Kolka, R. K.: Spatial characteristics of net methylmercury production hot spots in peatlands, Environ. Sci. Technol., 42(4), 1010–1016, doi:10.1021/es0704986, 2008.
Moreno, L. and Tsang, C. -F: Flow channeling in strongly heterogeneous porous media: A numerical study, Water Resour. Res., doi:10.1029/93WR02978, 1994.
Ritzi, R. W., Dai, Z., Dominic, D. F. and Rubin, Y. N.: Spatial correlation of permeability in cross-stratified sediment with hierarchical architecture, Water Resour. Res., doi:10.1029/2003WR002420, 2004.
Rubin, Y.: Prediction of tracer plume migration in disordered porous media by the method of conditional probabilities, Water Resour. Res., doi:10.1029/91WR00094, 1991.
Rubin, Y.: Applied Stochastic Hydrogeology, Oxford University Press, Oxford, UK., 2003.
Rubin, Y. and Dagan, G.: Conditional estimation of solute travel time in heterogeneous formations: Impact of transmissivity measurements, Water Resour. Res., doi:10.1029/91WR02759, 1992.
Rubin, Y. and Journel, A. G.: Simulation of non-Gaussian space random functions for modeling transport in groundwater, Water Resour. Res., doi:10.1029/91WR00838, 1991.
Rubin, Y., Mavko, G. and Harris, J.: Mapping permeability in heterogeneous aquifers using hydrologic and seismic data, Water Resour. Res., doi:10.1029/92WR00154, 1992.
Salandin, P. and Fiorotto, V.: Solute transport in highly heterogeneous aquifers, Water Resour. Res., 34(5), doi:10.1029/98WR00219, 1998.

Sassen, D. S., Hubbard, S. S., Bea, S. A., Chen, J., Spycher, N. and Denham, M. E.: Reactive facies: An approach for parameterizing field-scale reactive transport models using geophysical methods, Water Resour. Res., 48(10), doi:10.1029/2011WR011047, 2012.

Schwarz, G.: Estimating the Dimension of a Model, Ann. Stat., doi:10.1214/aos/1176344136, 1978.

Shrestha, N. K. and Wang, J.: Current and future hot-spots and hot-moments of nitrous oxide emission in a cold climate river basin, Environ. Pollut., 239, 648–660, doi:10.1016/j.envpol.2018.04.068, 2018.

Sørensen, R., Zinko, U. and Seibert, J.: On the calculation of the topographic wetness index: Evaluation of different methods based on field observations, Hydrol. Earth Syst. Sci., doi:10.5194/hess-10-101-2006, 2006.

USEPA: Risk Assessment Guidance for Superfund., 2001.

Vidon, P., Allan, C., Burns, D., Duval, T. P., Gurwick, N., Inamdar, S., Lowrance, R., Okay, J., Scott, D. and Sebestyen, S.: Hot spots and hot moments in riparian zones: Potential for improved water quality management, J. Am. Water Resour. Assoc., 46(2), 278–298, doi:10.1111/j.1752-1688.2010.00420.x, 2010.

Wainwright, H. M., Orozco, A. F., Bucker, M., Dafflon, B., Chen, J., Hubbard, S. S. and Williams, K. H.: Hierarchical Bayesian method for mapping biogeochemical hot spots using induced polarization imaging, Water Resour. Res., 51, 9127–9140, doi:10.1002/2014WR016259, 2015.

Wilson, A. and Rubin, Y.: Characterization of aquifer heterogeneity using indicator variables for solute concentrations, Water Resour. Res., 38(12), 19-1-19–12, doi:10.1029/2000wr000116, 2002.